LA-UR -82-3235

Backup for
NUREG-0937

Los Alamos National Laboratory is operated by the University of California for the United States Department of Energy under contract W-7405-ENG-36

TITLE: TRAC PD-2 Calculation of a Cold-Leg Small-Break in a Westinghouse 4-Loop Pressurized Water Reactor

AUTHOR(S): Gordon Willcutt
Jim Lime

SUBMITTED TO:

By acceptance of this article, the publisher recognizes that the U.S. Government retains a nonexclusive, royalty-free license to publish or reproduce the published form of this contribution, or to allow others to do so, for U.S. Government purposes

The Los Alamos National Laboratory requests that the publisher identify this article as work performed under the auspices of the U.S. Department of Energy

Los Alamos
Los Alamos National Laboratory
Los Alamos, New Mexico 87545

FO
ST
8301060444 830105
PDR NUREG
0937 C PDR

CONTENTS

FIGURES

FIGURES (Continued)

TABLES

TRAC-PD2 CALCULATION OF A COLD-LEG SMALL BREAK IN A WESTINGHOUSE FOUR-LOOP PRESSURIZED WATER REACTOR*

By

J. F. Lime and G. J. E. Willcutt, Jr.

ABSTRACT

In this report we present a TRAC-PD2 audit calculation of a 0.00186-m^2 (0.02-ft^2) cold-leg small break in a Westinghouse four-loop pressurized water reactor. Plant model assumptions and special code features are described, TRAC calculation results are presented, differences between the TRAC and Westinghouse results are discussed, and conclusions and recommendations are presented.

I. EXECUTIVE SUMMARY

We calculated a cold-leg small-break transient for a Westinghouse four-loop pressurized water reactor as requested by the Nuclear Regulatory Commission. We used the TRAC-PD2 computer code and a model of the ZION-1 plant for this analysis. We assumed a break size of 0.00186 m^2 (0.02 ft^2). We also assumed loss of offsite power at reactor-trip time. The loss of offsite power results in an immediate trip of the primary pumps, loss of main feedwater, closing of the turbine stop valves, and availability of only half the safety injection and auxiliary feedwater systems.

We calculated the transient out to 5000 s. The system transient behavior was characterized by an initial rapid decrease in primary pressure until it reached slightly above the steam generator secondary pressure. The system temporarily stabilized at that level until the loop seals cleared of liquid at about 2100 s. After the loop seals cleared, the pressure gradually decreased for the rest of the transient. The safety injection flow began exceeding the break flow at 4200 s.

There was no core uncovery during the transient. The void fractions in the upper level of the core remained well below 0.4 except for a brief period just before loop seal clearance, during which it peaked at 0.68. The peak cladding temperature never exceeded the steady-state value.

We compared the TRAC results to a Westinghouse calculation for the same break area. We found the calculated system behavior to be very similar but with some differences. The major difference is that Westinghouse shows a brief core

---

*Work performed under the auspices of the United States Nuclear Regulatory Commission.

uncovery while the TRAC calculation shows no core uncovery. This may be due to the lower safety injection flow assumed by Westinghouse.

We recommend the same calculation be performed using the improved TRAC-PF1 two-fluid code for small breaks. We also recommend the calculation be repeated using the lower safety injection flow assumed by Westinghouse.

II. INTRODUCTION

We calculated a cold-leg small-break transient for a Westinghouse four-loop pressurized water reactor (PWR) as requested by the Nuclear Regulatory Commission. We used the TRAC-PD2 computer code and a model of the ZION-1 PWR for this analysis. The break size of 0.00186 m^2 (0.02 ft^2) and other PWR model assumptions corresponded to a Westinghouse calculation. We calculated the transient out to 5000 s. Sec. III of this document describes the PWR model, special features of the code, and initial conditions. Sec. IV presents the TRAC calculation results and a comparison of the TRAC and Westinghouse results. Finally, Sec. V and VI present conclusions and recommendations.

III. MODEL DESCRIPTION

A. Nodalization

Figure 1 shows a sketch of the TRAC model used. The small break is located in the cold leg of loop B, downstream of the pump and safety injection point. The pressurizer is also located in loop B. The three intact loops are modeled as one combined loop, referred to as loop ACD in this analysis. We divided the vessel into eight axial levels, two theta segments, and two radial rings. The core is modeled with four axial levels. On the secondary side of the steam generators, we also modeled the steam lines leading outside the containment building and the secondary safety valves. We also modeled the primary loop seals between the steam generator outlets and the primary coolant pumps. There are a total of 32 3-D vessel cells and 132 1-D cells, 80 in the primary loops and 52 in the secondary side. Geometry and other plant data were obtained from the ZION FSAR and from other ZION data sources.

B. TRAC Code Special Features

We used the TRAC-PD2 computer code with modifications to add an auxiliary feedwater inlet to the steam generator components and to include reactivity feedback and decay power calculations. We also modified the 1-D drift-flux slip correlations to improve the liquid-vapor mixing between cells at the very low flows encountered in small-break transients. The TRAC-PD2 code version we used also includes several other minor improvements and corrections.

C. Initial Conditions and Boundary Assumptions

Table I summarizes the initial steady-state flow conditions and boundary assumptions used in this analysis. The initial conditions agree reasonably well with FSAR data. We also assumed loss of offsite power at reactor-trip time, which is consistent with the Westinghouse calculation. The offsite power loss results in an immediate trip of the primary pumps, loss of main feedwater, closing of the turbine stop valves, and availability of only half the safety injection and auxiliary feedwater systems. Furthermore, we assumed a 25-s and 60-s delay in delivery of the safety injection flow and of the auxiliary feedwater flow, respectively. The auxiliary feedwater remains on for 3000 s of the transient. Table II shows the pressure-dependent safety injection flow and the auxiliary feedwater flow used in the calculation.

IV. CALCULATION RESULTS

A. TRAC Results

This section presents the small-break transient results. Table III summarizes the significant events of the transient. Time-history plots of the system pressures, temperatures, mass flows, void fractions, and other data are presented.

Figure 2 shows the pressurizer and steam generator secondary pressures. The transient was characterized by a rapid depressurization of the primary system in the first 500 s. Between 500 and 1500 s, the pressure temporarily stabilized at slightly above the steam generator secondary pressure. The steam generator secondary pressure rapidly increased to the secondary safety valve setpoint following loss of main feedwater at the reactor-trip time and remained at that level until approximately 1700 s. At 1500 s, the primary pressure began to increase until the primary loop seals cleared of liquid at about 2100 s. After the loop seals cleared, a gradual depressurization occurred for the rest of the transient. The secondary pressure also decreased until the auxiliary feedwater was turned off at 3129 s, after 3000 s of operation as assumed in the Westinghouse calculation. The secondary pressure then remained relatively constant for the rest of the transient.

Figure 3 shows the void fractions in the upper two levels of the core and in the upper plenum. The void fraction in level 6, the top level of the core, remained well below 0.4 except for a brief period between 2200 s and 2400 s, during which it peaked at 0.68. To determine whether any core uncovery occurred, we renoded the top core level into three smaller levels and recomputed the transient between 2000 s and 2500 s. In the renoded case, the void fraction in the topmost core level never exceeded 0.8. Figure 4 shows the core level 6 liquid temperature. Peak cladding temperatures never exceeded the steady-state value during the transient period.

The vessel liquid mass inventory is shown in Fig. 5. Figure 6 shows the break flow and the total safety injection flow. The safety injection flow began exceeding the break flow at about 4200 s. However, the vessel liquid-mass inventory actually began increasing at about 3700 s from condensing steam.

The clearing of liquid in the primary loop seals had an important effect. Before loop seal clearance, the break flow was essentially all liquid which resulted in a high mass loss. Once the loop seals cleared, an open path was formed between the core upper plenum and the break, allowing the upper-plenum high-vapor mixture to escape and exit out the break. The path was not a direct one because the loop seal in the break loop never cleared. Instead, the flow escaped in a roundabout way, through the intact loops, through the downcomer annulus, and into the break cold leg from the vessel side. The high volumetric flow out the break resulted in a marked decrease in break mass flow and in pressure. Figure 7 shows the void fraction of the flow entering the break. The flow reaching the break was never completely steam because of partial condensation in the steam generator tubes.

Figure 8 shows the pressurizer water level. The pressurizer emptied very rapidly and remained nearly empty except briefly just before loop seal clearance.

Figures 9 and 10 show the primary mass flow for loops B and ACD. Flow circulation ceased at approximately 2200 s except for the upper plenum vapor flow escaping out the break. A better indication of the flow circulation after 2200 s is given by the mixture velocity shown in Fig. 11 for loop B and Fig. 12 for loop ACD. Flow was never re-established in loop B because the loop seal in that loop never cleared.

Hot- and cold-leg temperatures are shown in Fig. 13 for loop B and in Fig. 14 for loop ACD. The hot- and cold-leg temperatures approached saturation temperature as the loops drained. The decrease in cold-leg temperature between 1100 s and 2100 s was due to the accumulation of safety injection flow when very low loop flow rates were occurring.

The steam generator primary and secondary temperatures are shown in Fig. 15 for loop B and in Fig. 16 for loop ACD. After 3500 s the primary temperature was lower than the secondary temperature, resulting in heat transfer from the secondary to the primary. However, the heat transfer was small and had little or no effect on the primary system response.

Voiding in the primary loops is shown by the next set of plots. Figures 17 through 20 show the void fractions in loop B at the hot-leg inlet, the top of the steam generator, the bottom of the loop seal, and the cold-leg outlet. Figures 21 through 24 show the same void fractions for loop ACD. Note the difference in loop seal void fraction between loop B (Fig. 19) and loop ACD (Fig. 23).

The steam generator secondary water mass inventory is shown in Fig. 25. There was a depletion in water mass in the first 300 s after which the water mass inventory began increasing from the addition of auxiliary feedwater. The feedwater came on at 129 s and remained on for 3000 s. There was more secondary boiloff in loop B because of the higher primary mass flow in this loop as a result of the break. Figure 26 shows the void fraction in the secondary cell containing the top of the tube bundle, giving an indication of the water level reached. Figures 27 and 28 show the mass flow out the safety valves for loop B and ACD. The auxiliary feedwater flow is also shown in these figures.

B. Comparison of TRAC and Westinghouse Calculations

When we compared the TRAC and Westinghouse calculation results, both calculations showed the same general system behavior. There was an initial rapid pressure decrease with a leveling off at slightly above secondary pressure until the loop seals cleared, and then a gradual depressurization thereafter. However, the results differed in four areas:

(1) The Westinghouse results showed a brief core uncovery just before loop seal clearance. The TRAC results showed a brief increase in void fraction in the upper level of the core but no core uncovery.

(2) The Westinghouse results showed the loop seals clearing at 1800 s. The TRAC results showed the loop seals clearing at 2100 s.

(3) The Westinghouse results showed the break flow to be all steam once the loop seals clear. The TRAC results showed the break flow to be two-phase with a maximum void fraction of 0.69.

(4) The Westinghouse results showed the primary and secondary pressures remaining relatively constant after the auxiliary feedwater was turned off. The TRAC results showed the secondary pressure to remain constant, but the primary pressure to decrease continually after the auxiliary feedwater was turned off.

We also found the Westinghouse safety injection flow to be much lower than that used in TRAC, approximately 35 to 45 per cent lower depending on pressure. Our safety injection flow rates were based on one-half the full system flow rates given in the FSAR. We also checked the integrated break flow of the two calculations and found them to agree up to 1500 s. The first two differences noted above may be due to the difference in safety injection flow while the latter two differences may be due to differences in thermal-hydraulic modeling methods.

V. CONCLUSIONS

We completed a TRAC-PD2 calculation of a cold-leg small-break transient for a Westinghouse four-loop PWR. We compared the results to a Westinghouse calculation for the same size break. We found the calculated system behavior to be very similar but with some differences. The major difference is that Westinghouse shows a brief core uncovery while the TRAC calculation shows no core uncovery. This may be due to the lower safety injection flow assumed by Westinghouse.

VI. RECOMMENDATIONS

We recommend the same calculation be performed using the improved TRAC-PF1 two-fluid code for small breaks. We also recommend the calculation be repeated using the lower safety injection flow assumed by Westinghouse.

TABLE I

INITIAL CONDITIONS AND SETPOINTS

Parameter	Value
Reactor Power	3238 MW
Primary Pressure	15.4 MPa
Core Inlet Temperature	550.4 K
Core Outlet Temperature	585.7 K
Mass Flow (per loop)	4260 kg/s
Secondary Pressure	5.0 MPa
Feedwater Temperature	495.5 K
Steam Outlet Temperature	537.1 K
Feedwater Flow (per loop)	441.0 kg/s
Low Pressure Reactor Trip Setpoint	11.72 MPa
Steam Generator Safety Valve	
Valve Area (full open)	0.016 m^2
Open Setpoint	7.14 MPa
Close Setpoint	7.03 MPa

TABLE II

SAFETY INJECTION AND AUXILIARY FEEDWATER FLOW

1. Safety Injection Flow

One-half system capability (one charging pump and one safety injection pump) is assumed available with a 25-s delay in flow delivery after actuation signal.

Primary Pressure (MPa)	Total SI Mass Flow (kg/s)
0.0	58.967
2.76	52.617
5.52	45.353
8.27	35.380
10.45	21.772
12.41	19.051
13.79	16.329
15.17	12.701
16.55	7.711
17.93	0.0

2. Auxiliary Feedwater Flow

One-half system capacity (450 gpm or 28 kg/s) is available delivered to all four steam generators 60 s after reactor trip and loss of main feedwater. The auxiliary feedwater is assumed to remain on for 3000 s after initiation.

TABLE III

SUMMARY OF TRANSIENT EVENTS

Event	Time(s)
1. Break occurs.	0.0
2. Reactor trip signal, RCS pumps trip, loss of feedwater, and turbine stop valves close.	69.1
3. Reactor scrammed.	69.7
4. Safety injection flow initiated.	94.1
5. Auxiliary feedwater flow initiated.	129.1
6. Steam generator safety valves open.	150.0
7. Primary loop seals clear.	2100.0
8. Auxiliary feedwater flow stopped.	3129.0
9. Primary pressure drops below secondary pressure.	3500.0
10. Vessel liquid mass inventory starts to increase.	3700.0
11. Safety injection flow exceeds break flow.	4200.0

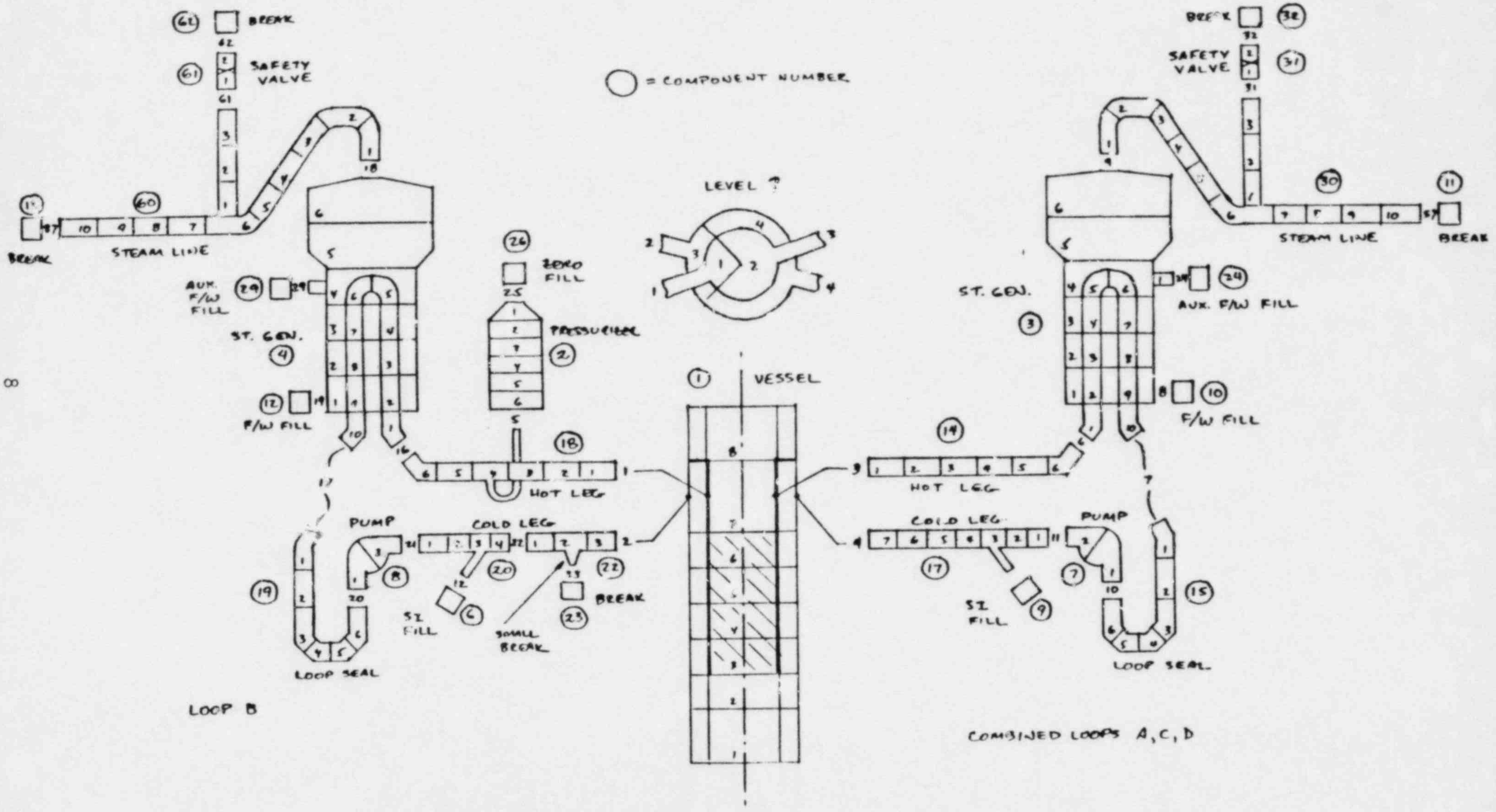

Fig. 1.
TRAC model of ZION-1 PWR.

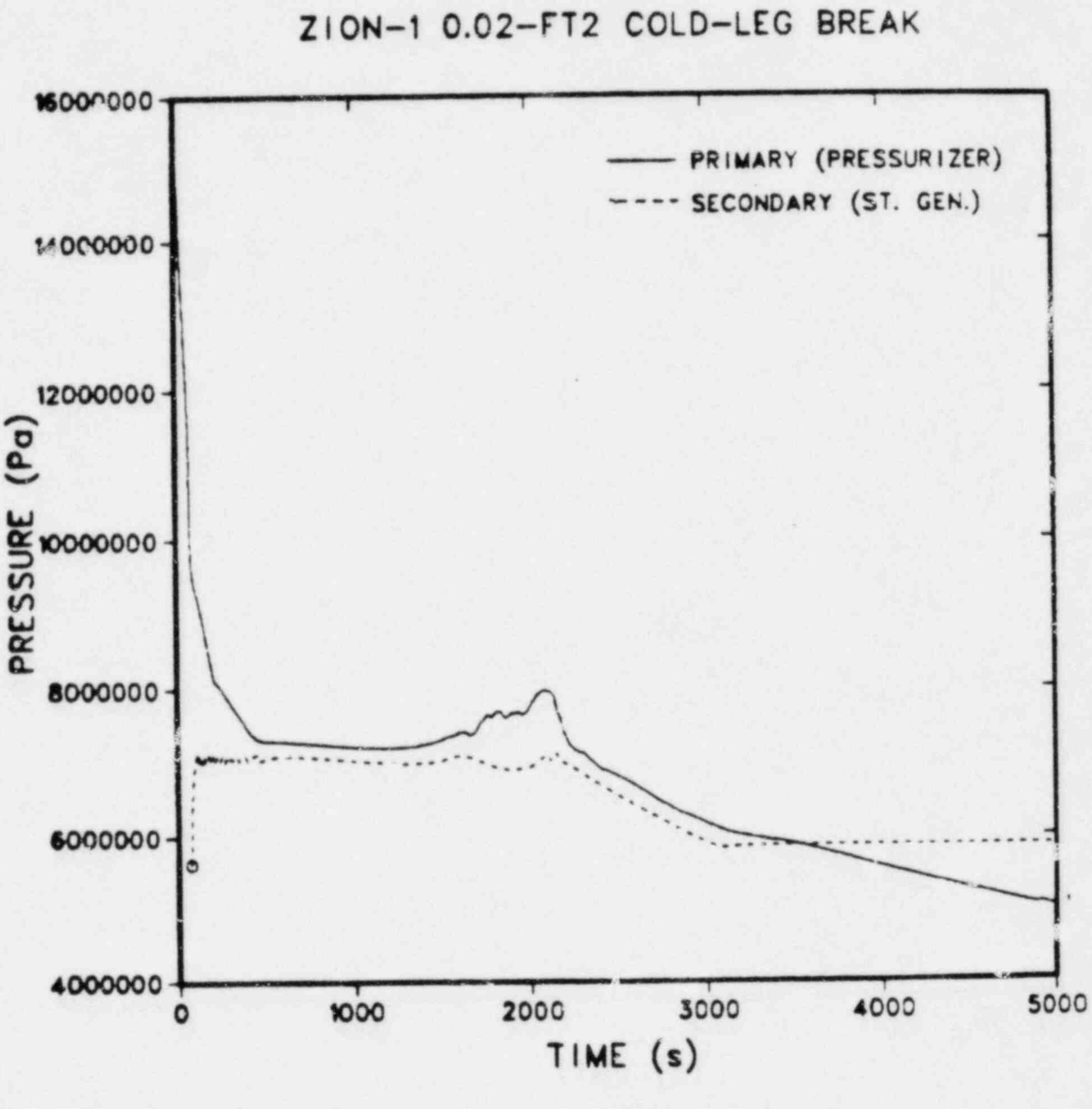

Fig. 2.
System primary and secondary pressures.

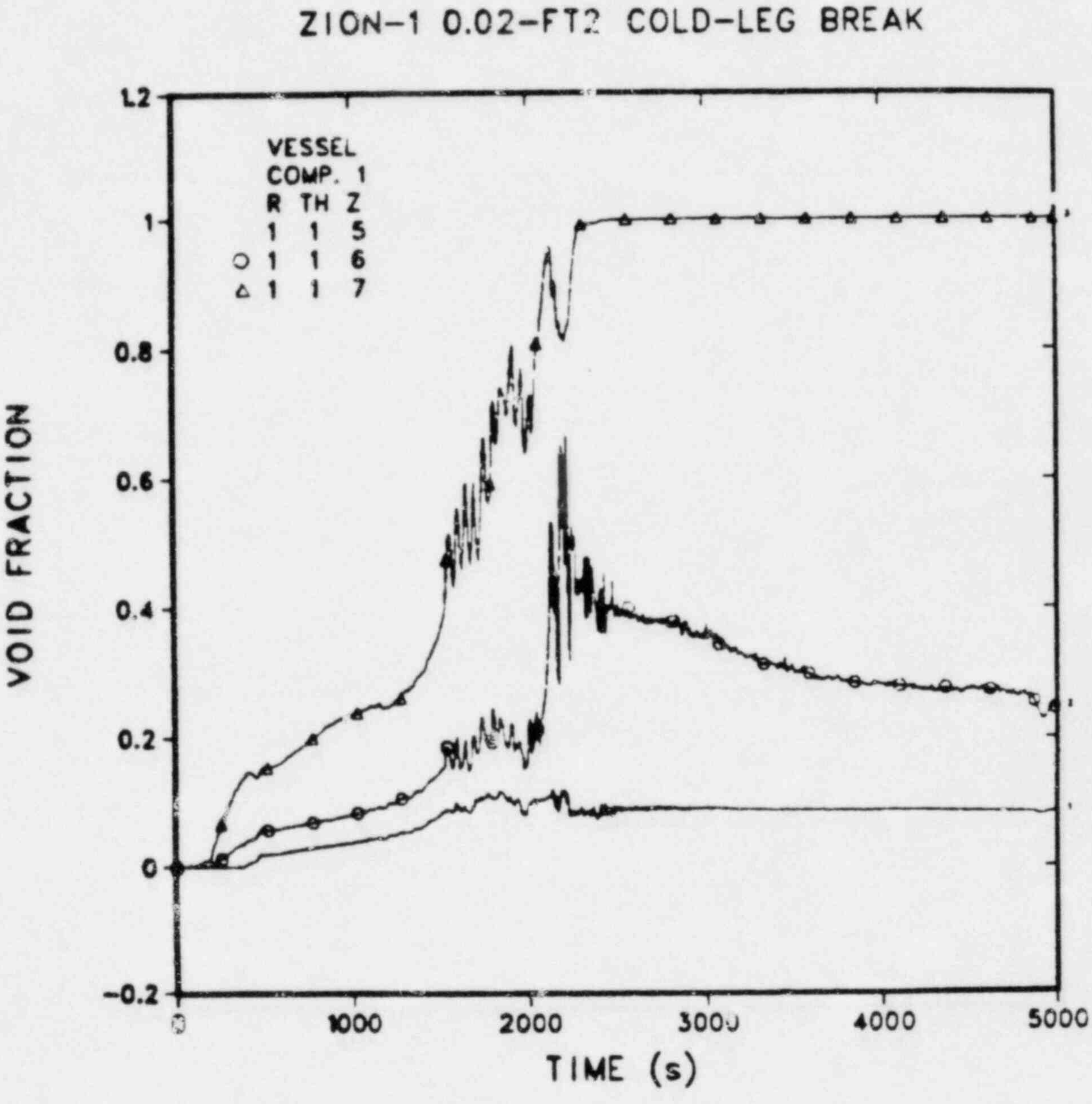

Fig. 3.
Core and upper plenum void fractions.

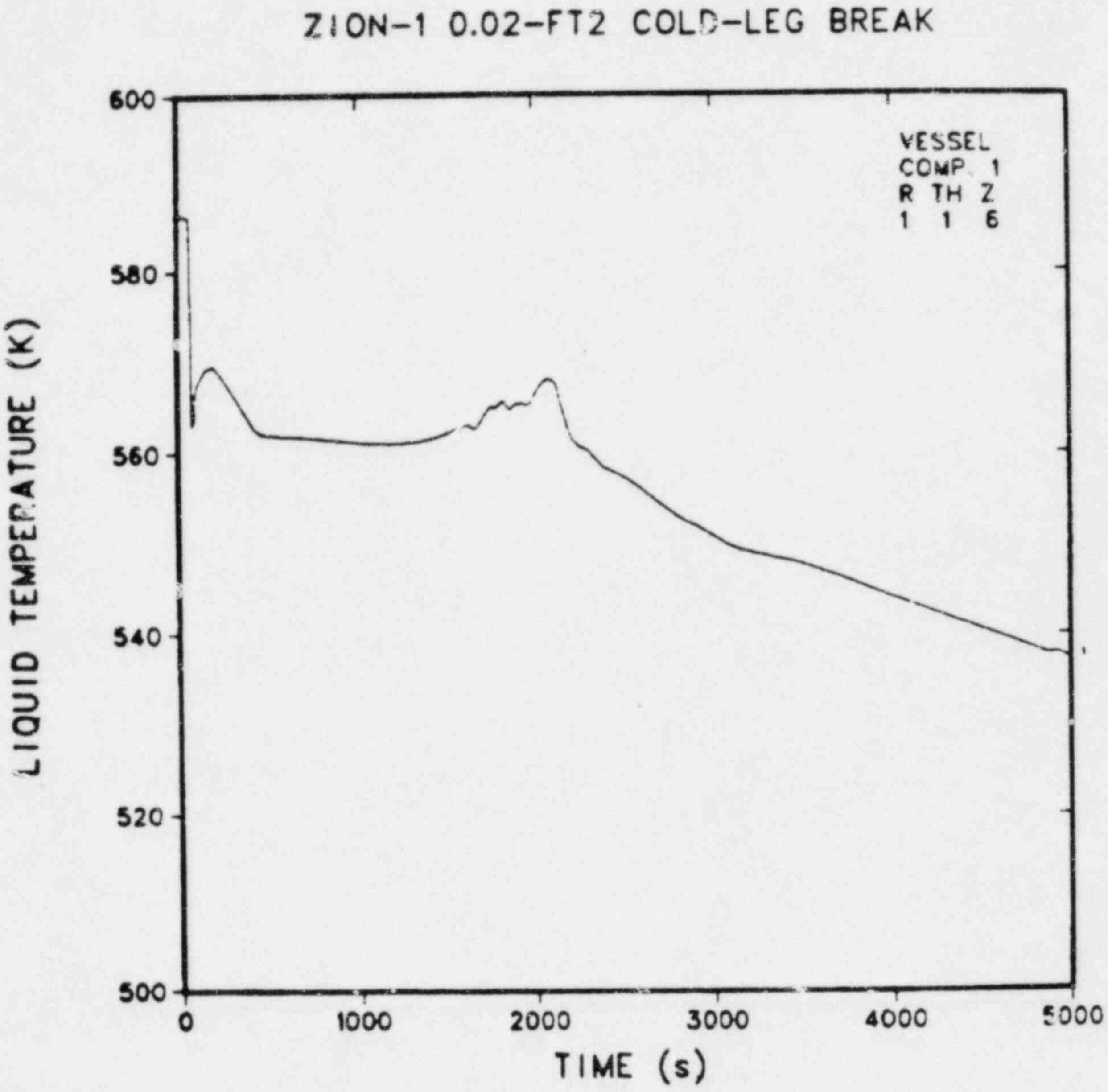

Fig. 4.
Core liquid temperature in level 6.

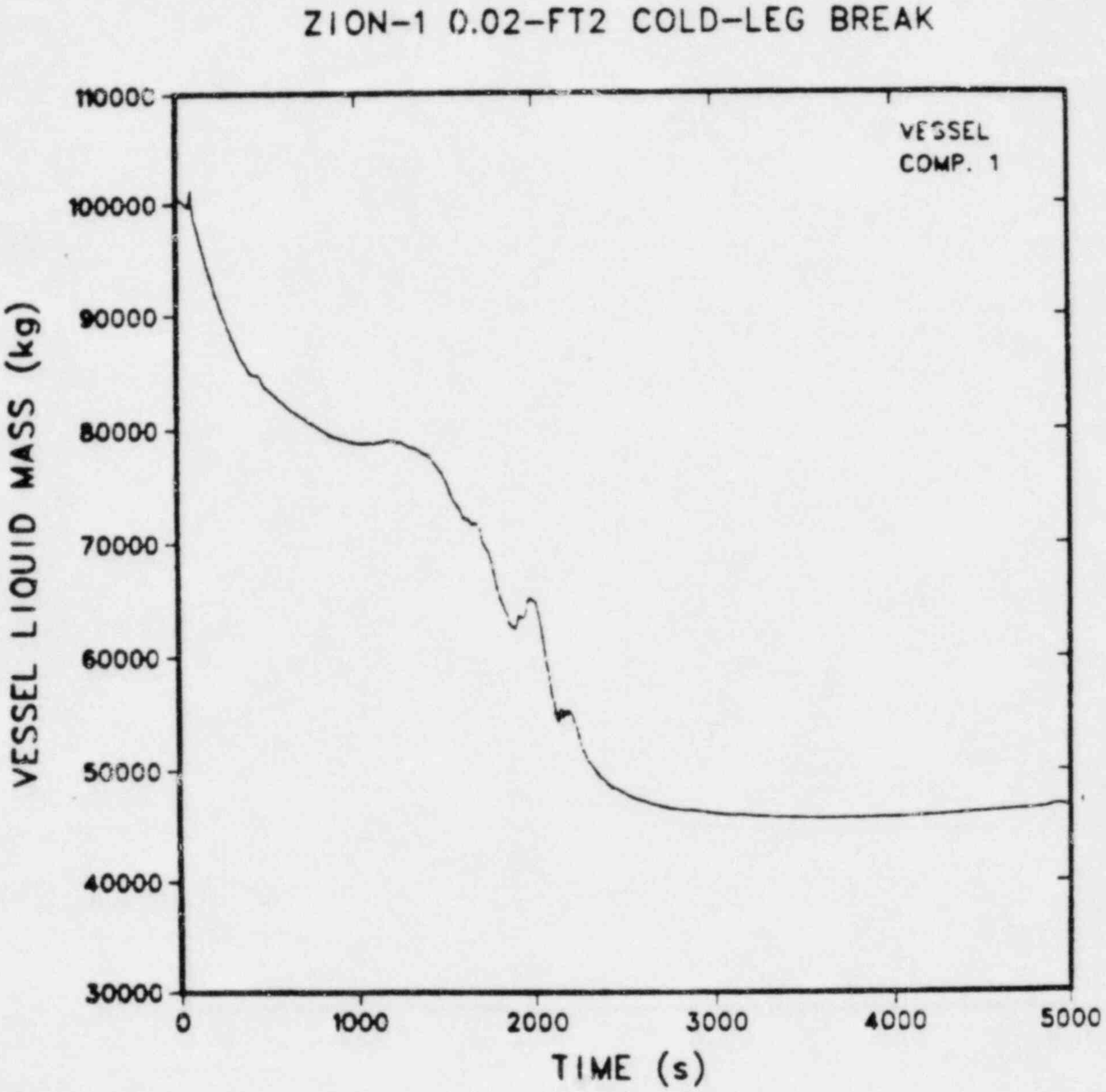

Fig. 5.
Vessel liquid mass inventory.

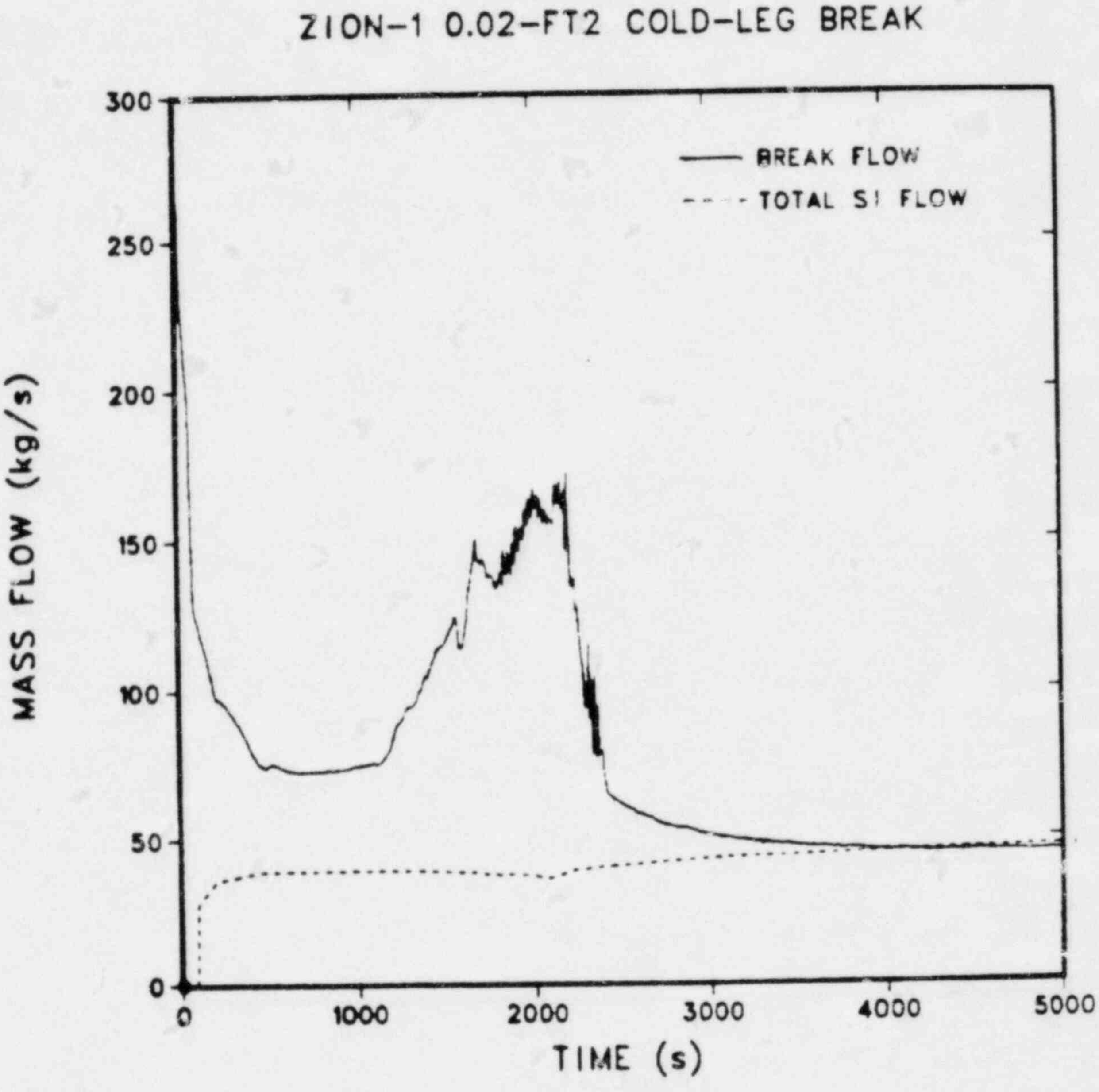

Fig. 6.
Break flow and safety injection flow.

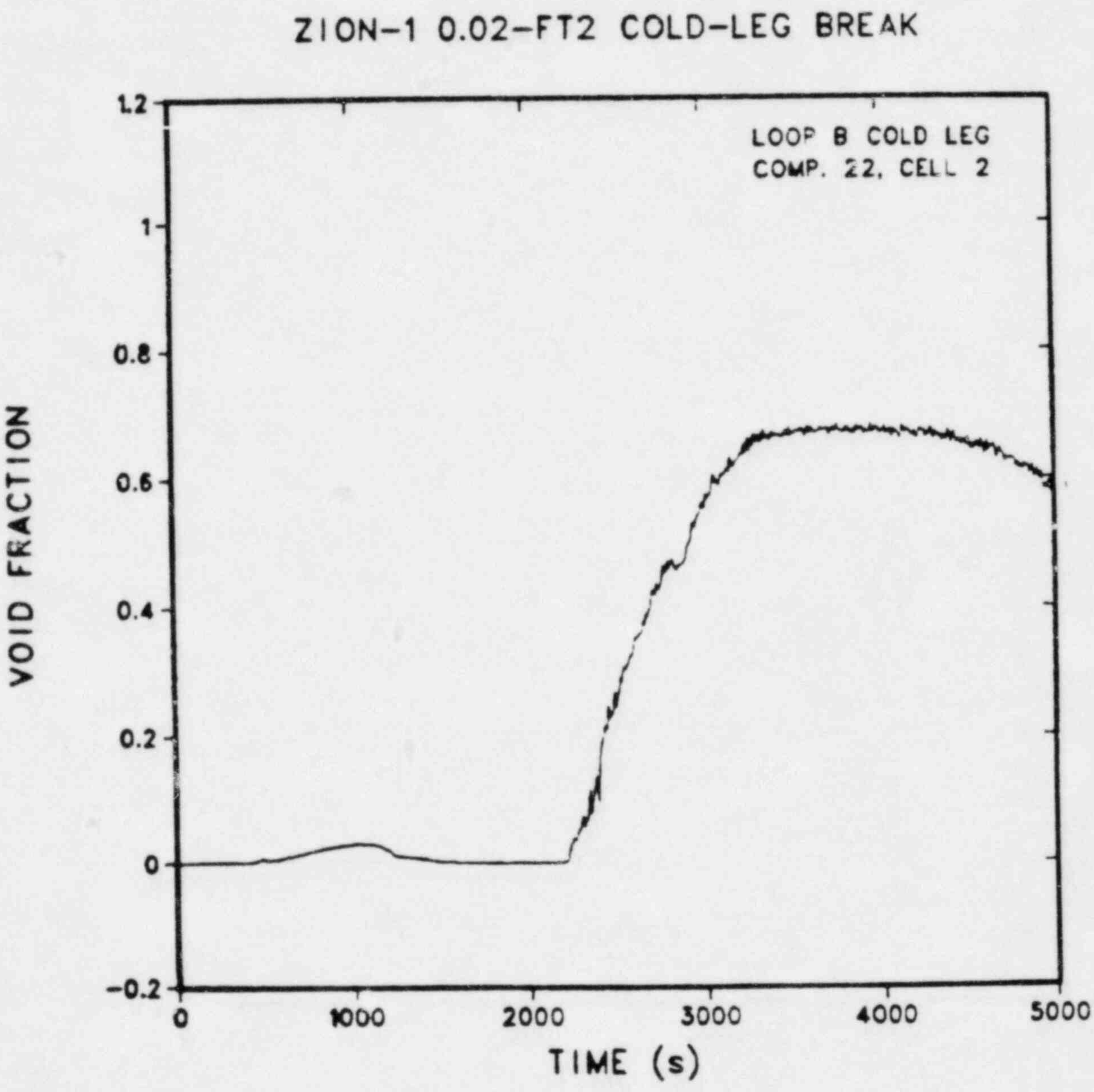

Fig. 7.
Void fraction of flow entering break.

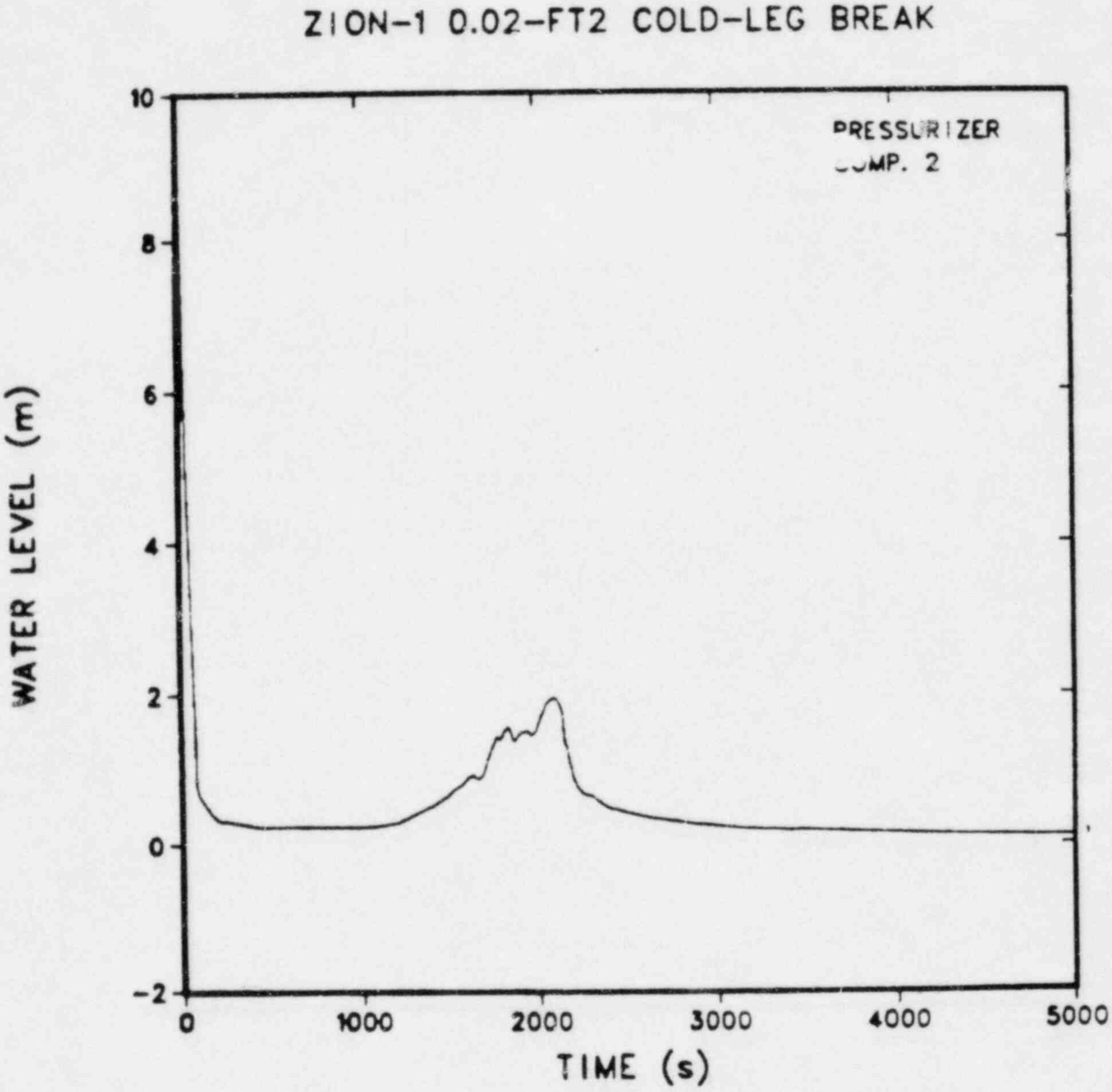

Fig. 8.
Pressurizer water level.

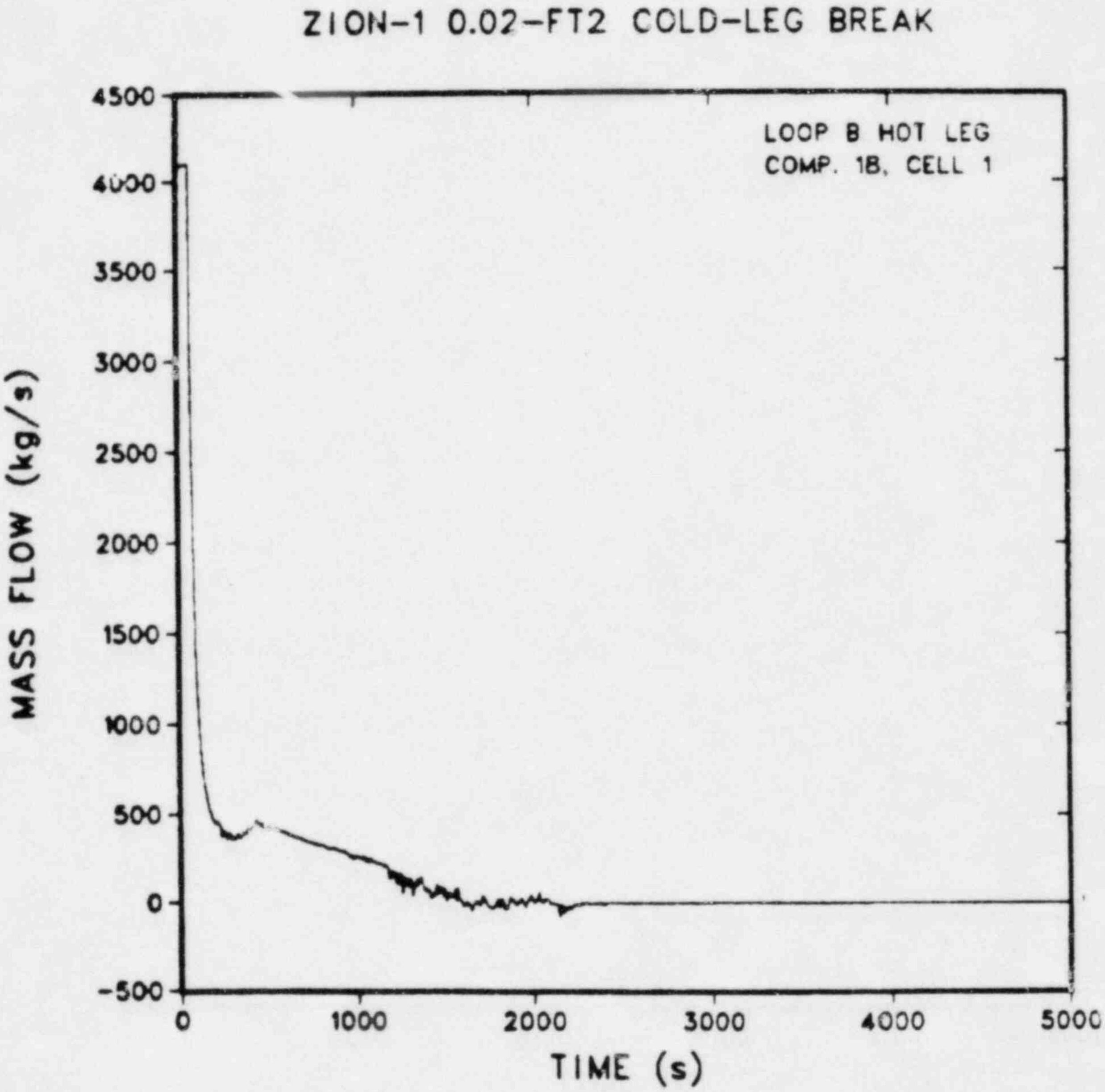

Fig. 9.
Loop B primary mass flow.

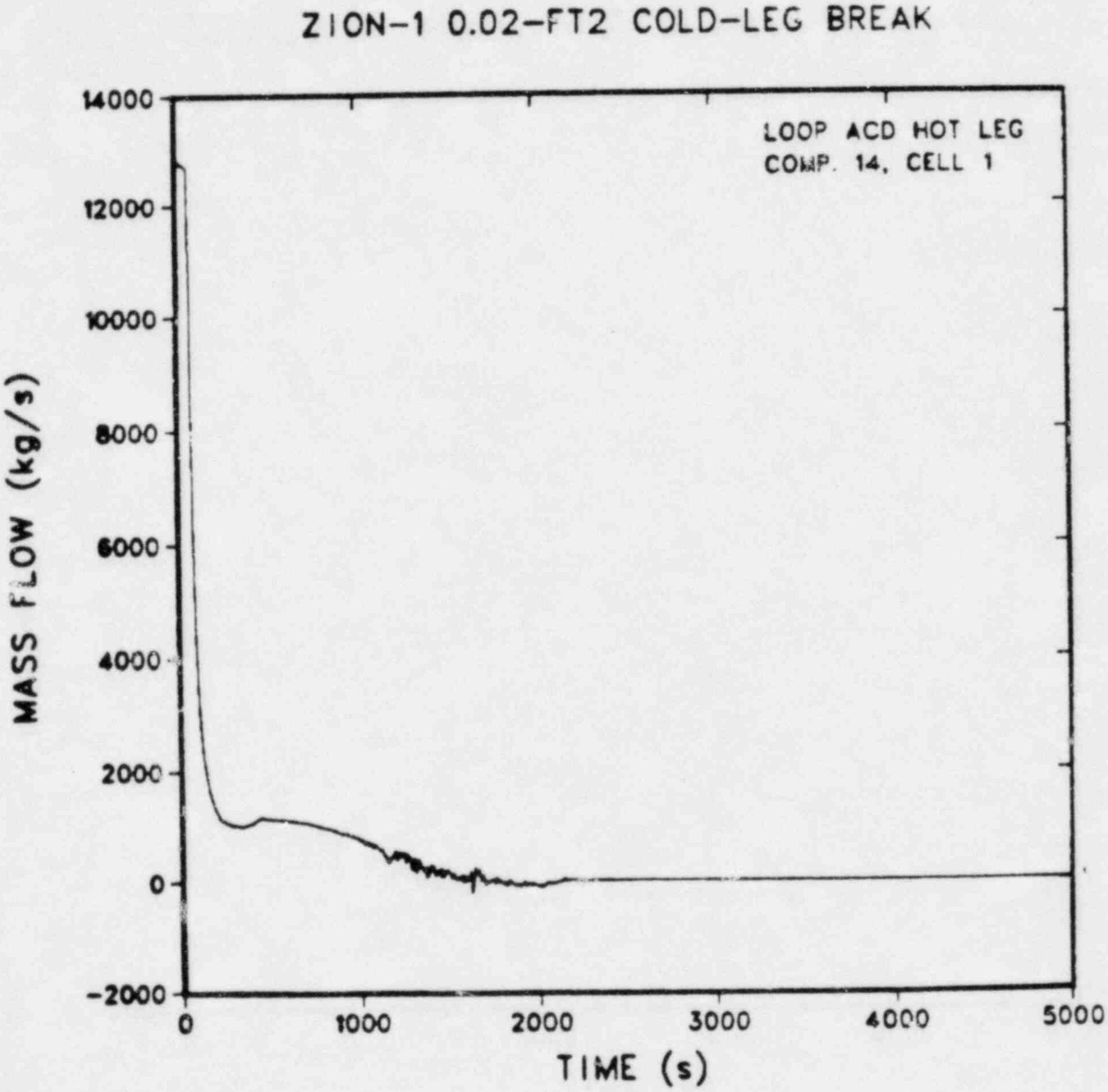

Fig. 10.
Loop ACD primary mass flow.

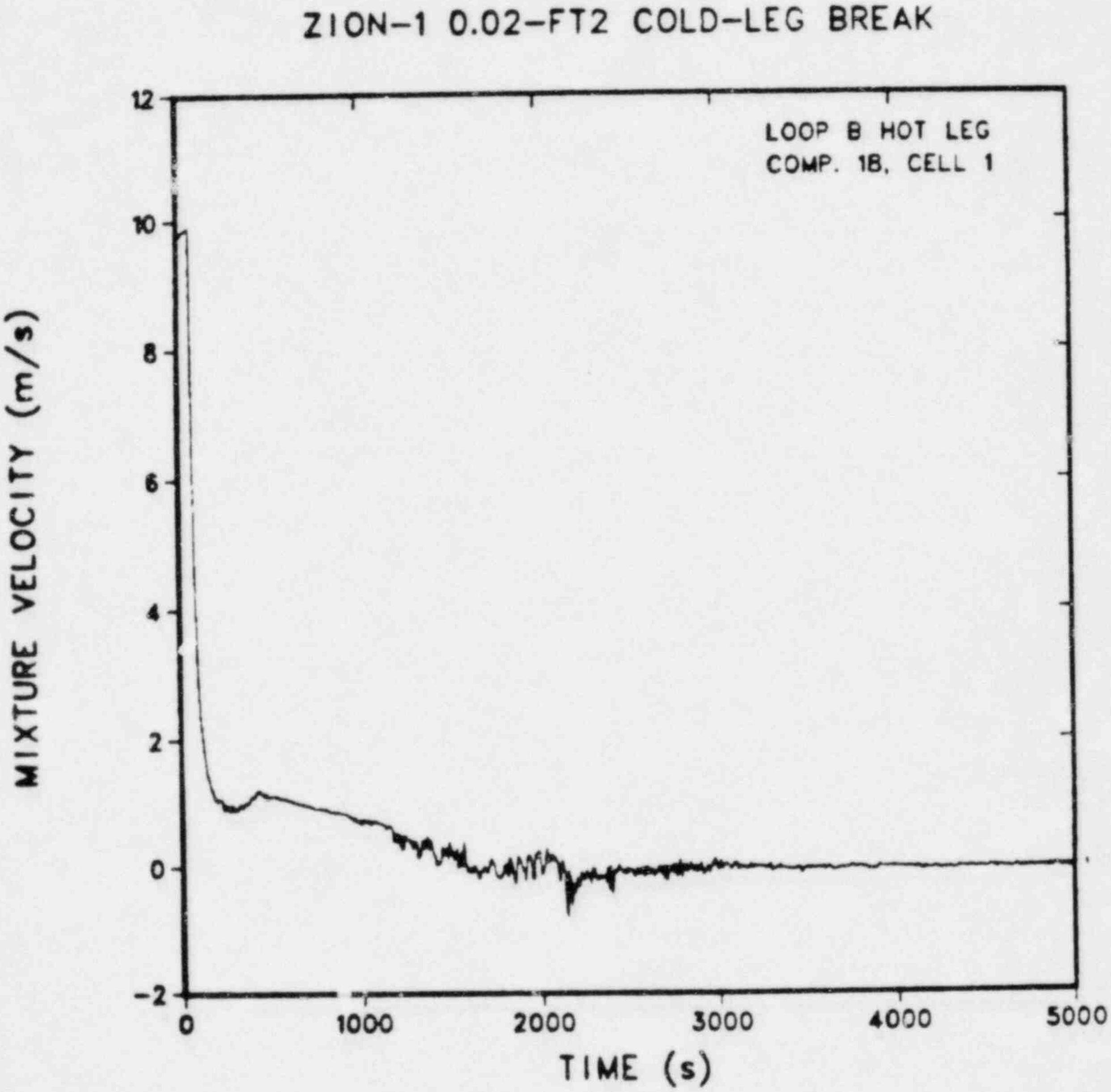

Fig. 11.
Loop B mixture velocity.

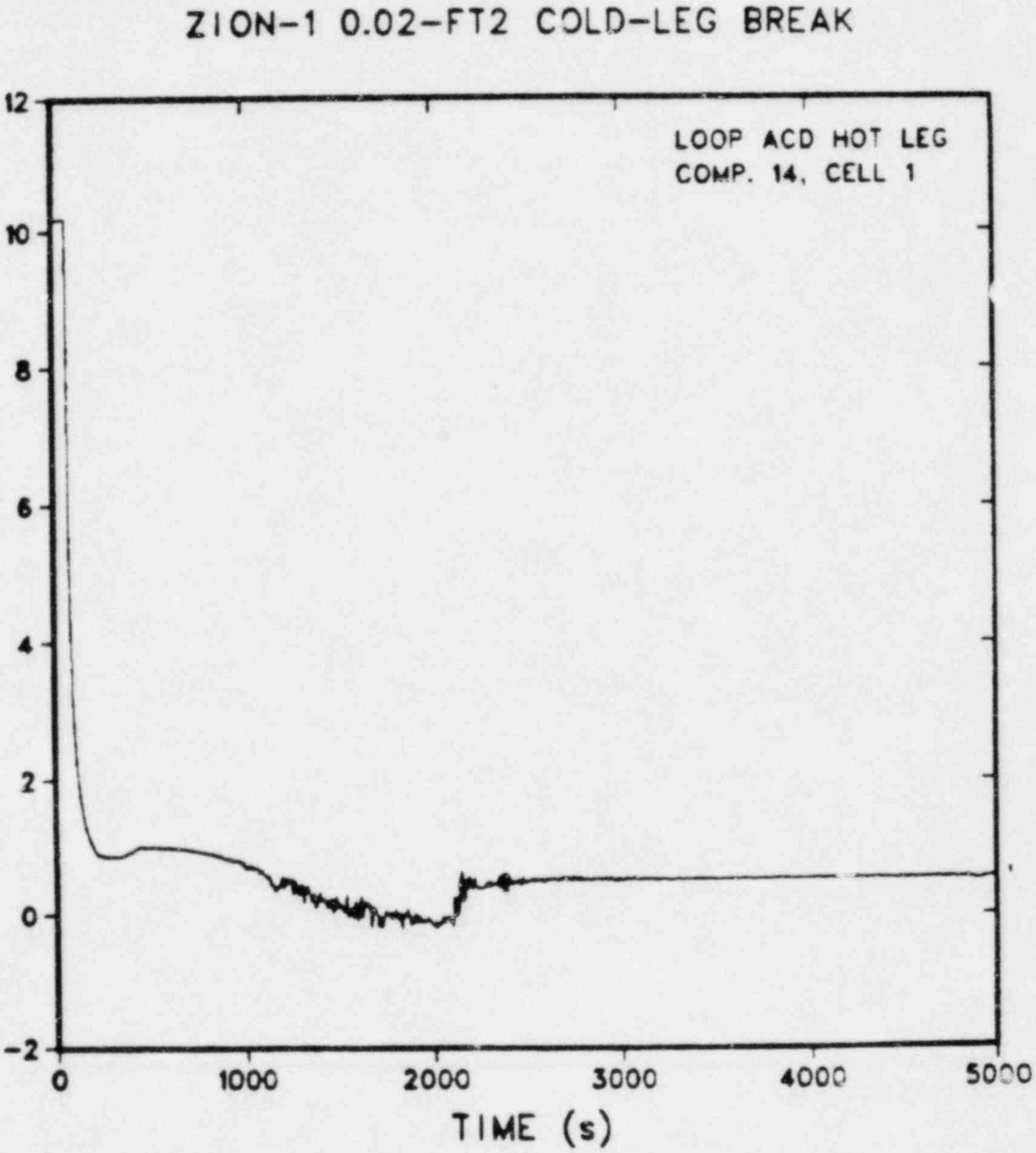

Fig. 12.
Loop ACD mixture velocity.

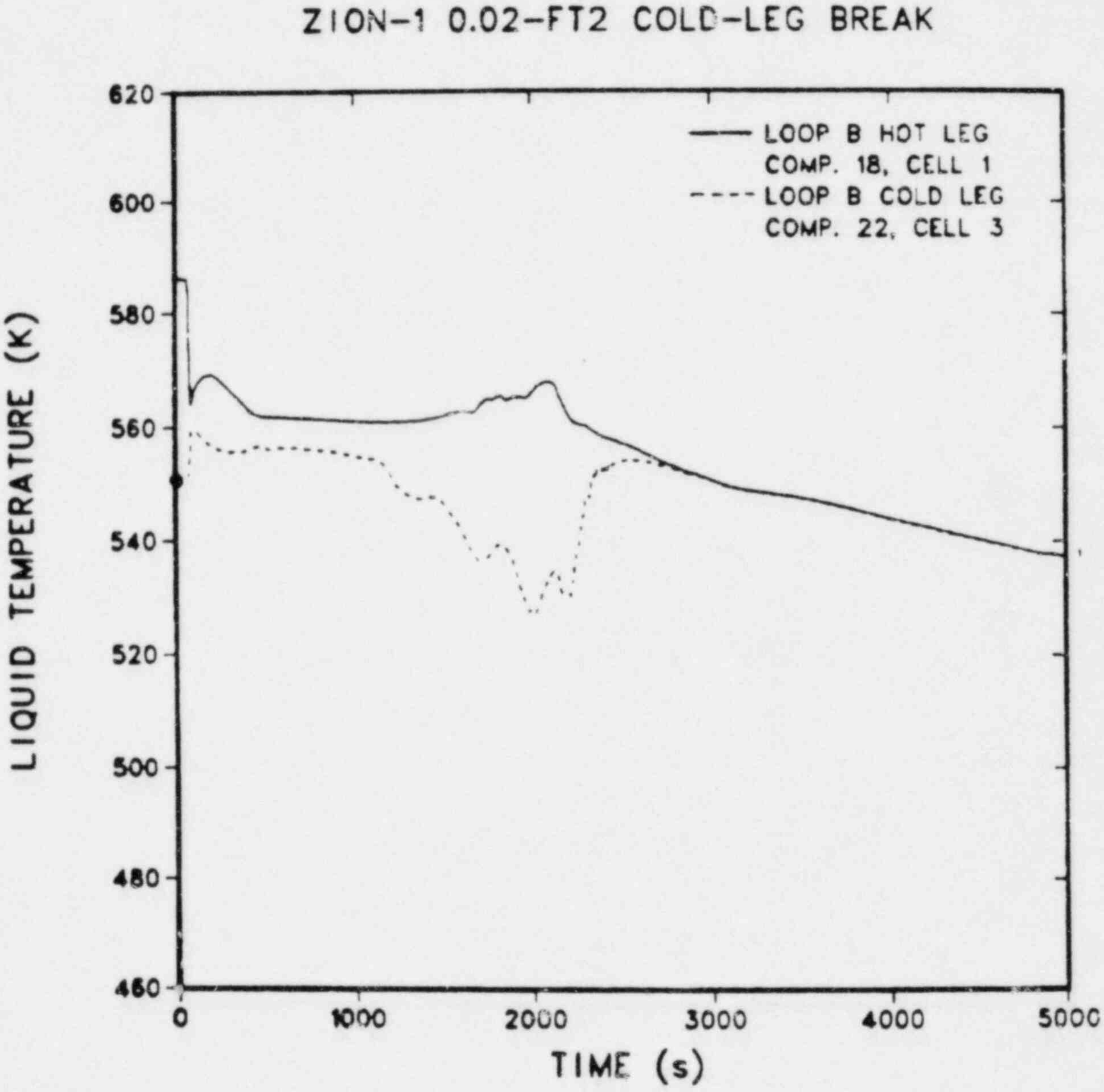

Fig. 13.
Loop B hot- and cold-leg temperatures.

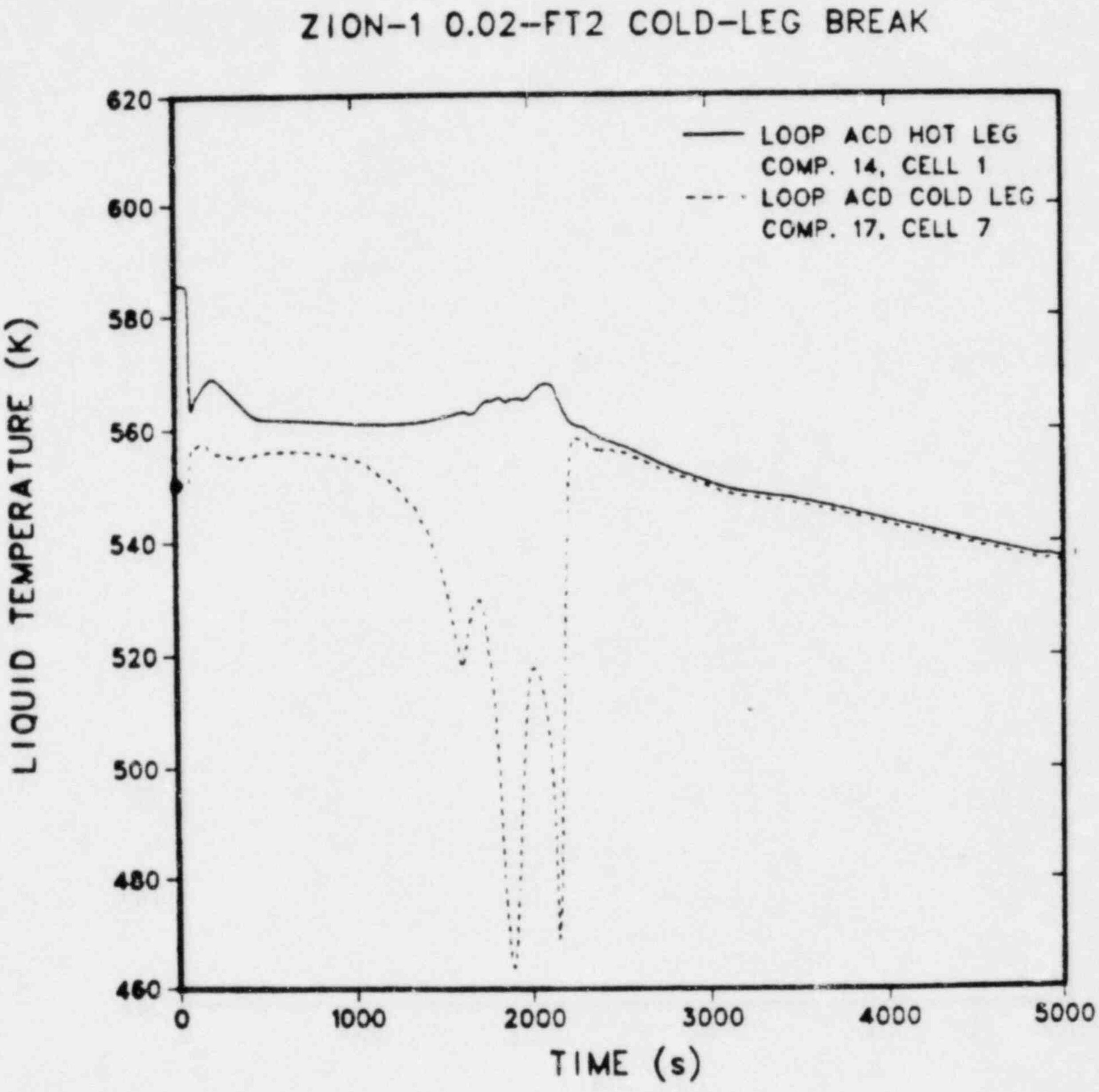

Fig. 14.
Loop ACD hot- and cold-leg temperatures.

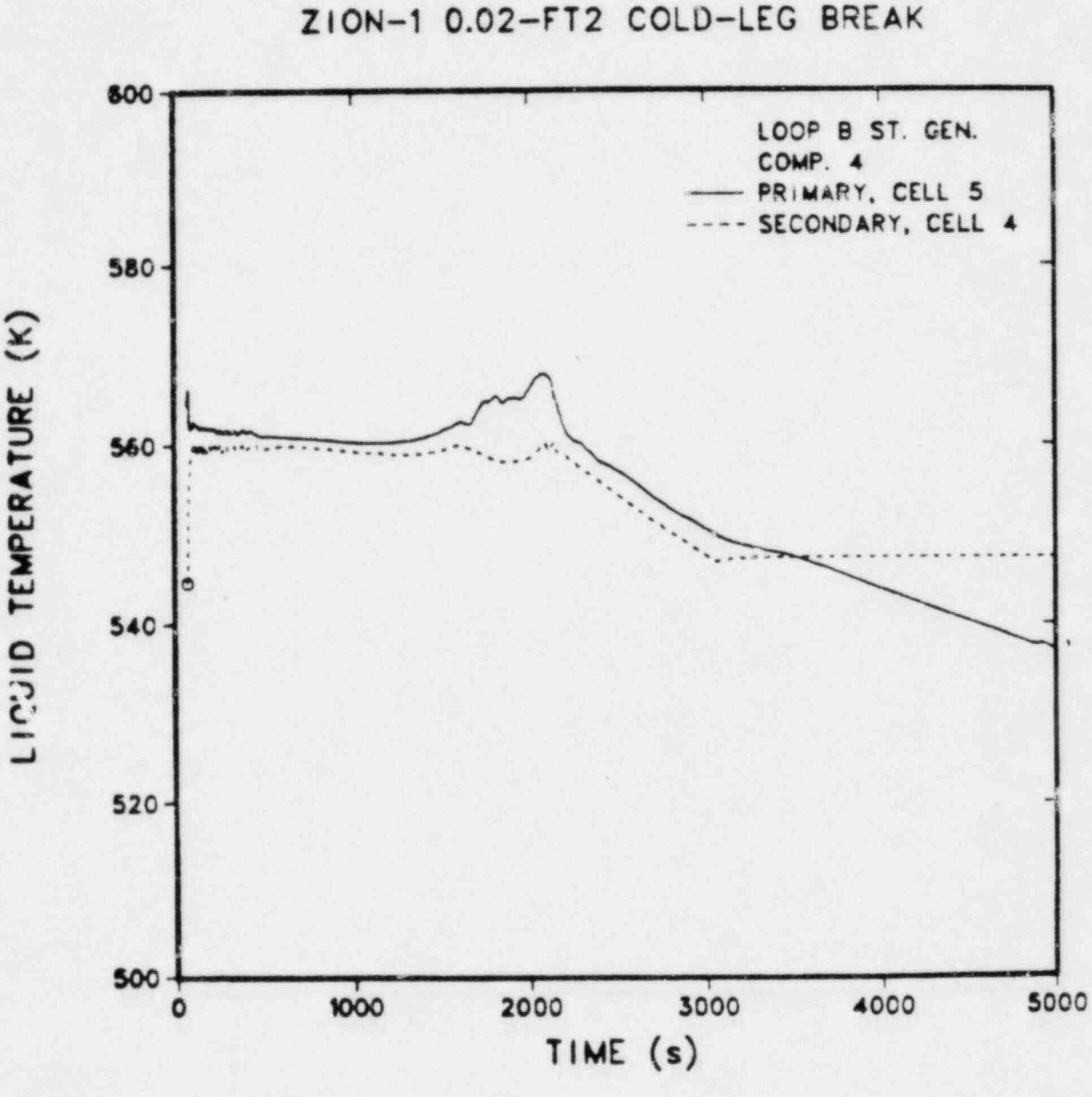

Fig. 15.
Loop B steam generator primary and secondary temperatures.

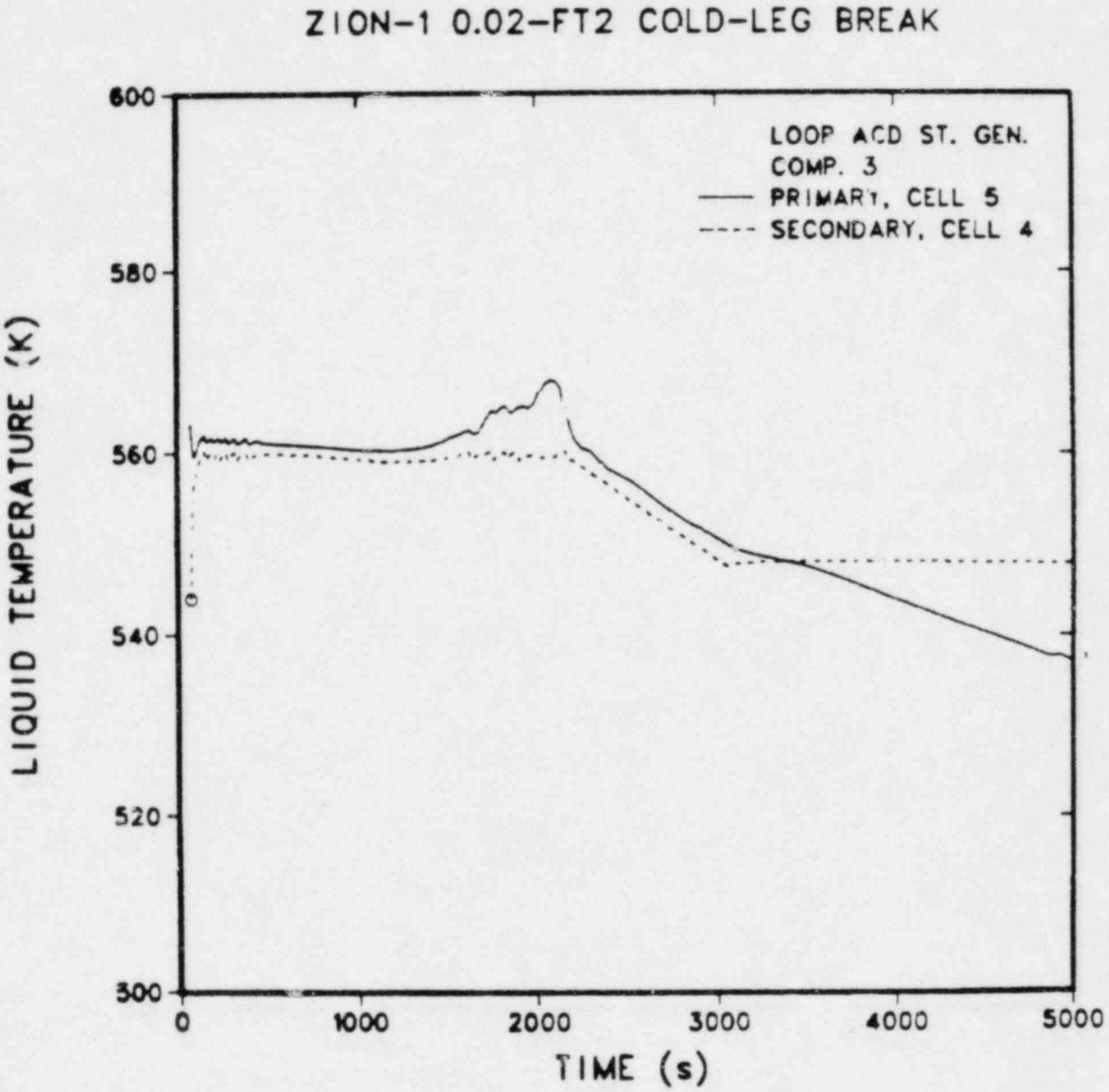

Fig. 16.
Loop ACD steam generator primary and secondary temperatures.

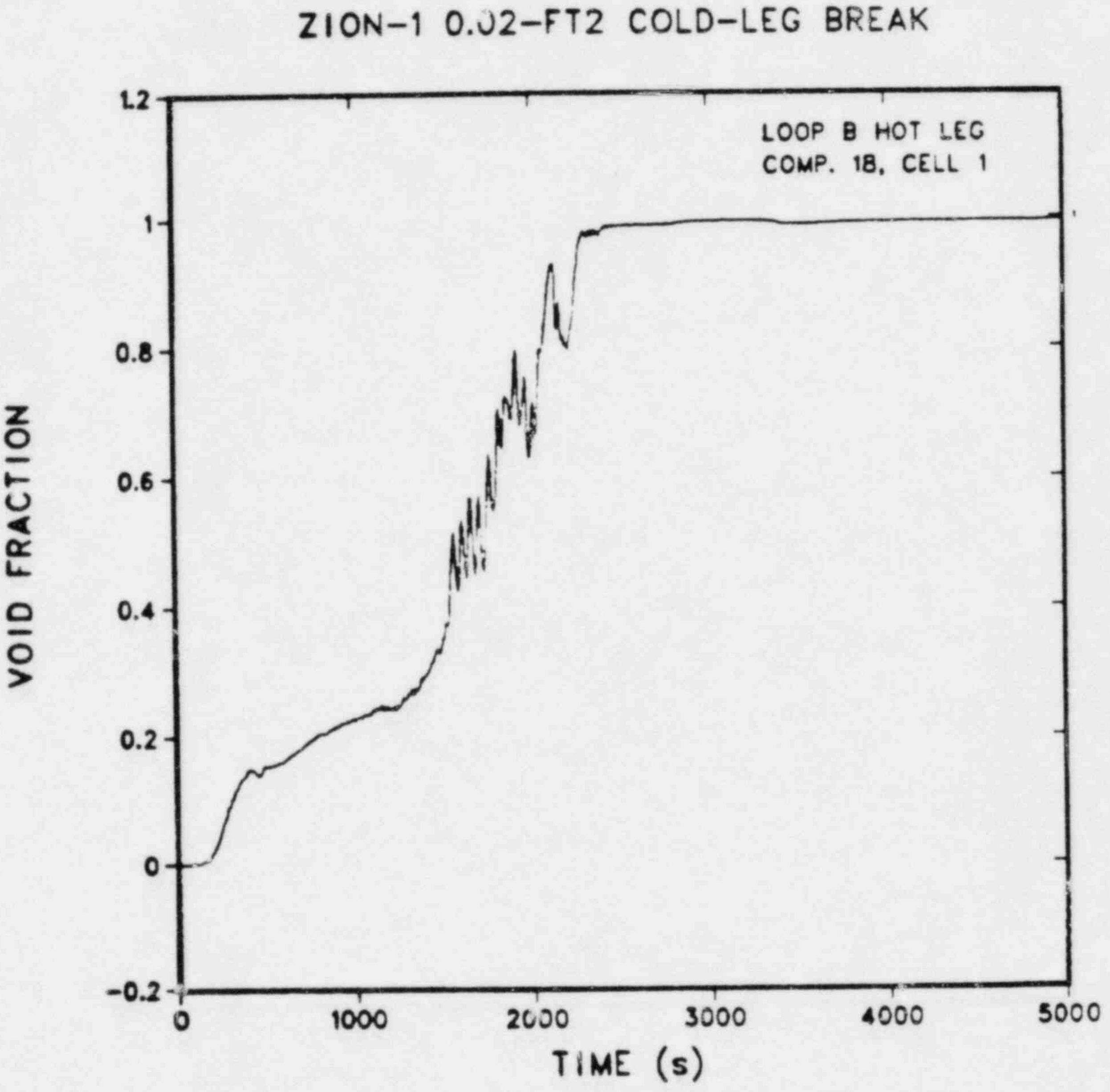

Fig. 17.
Loop B hot-leg void fraction.

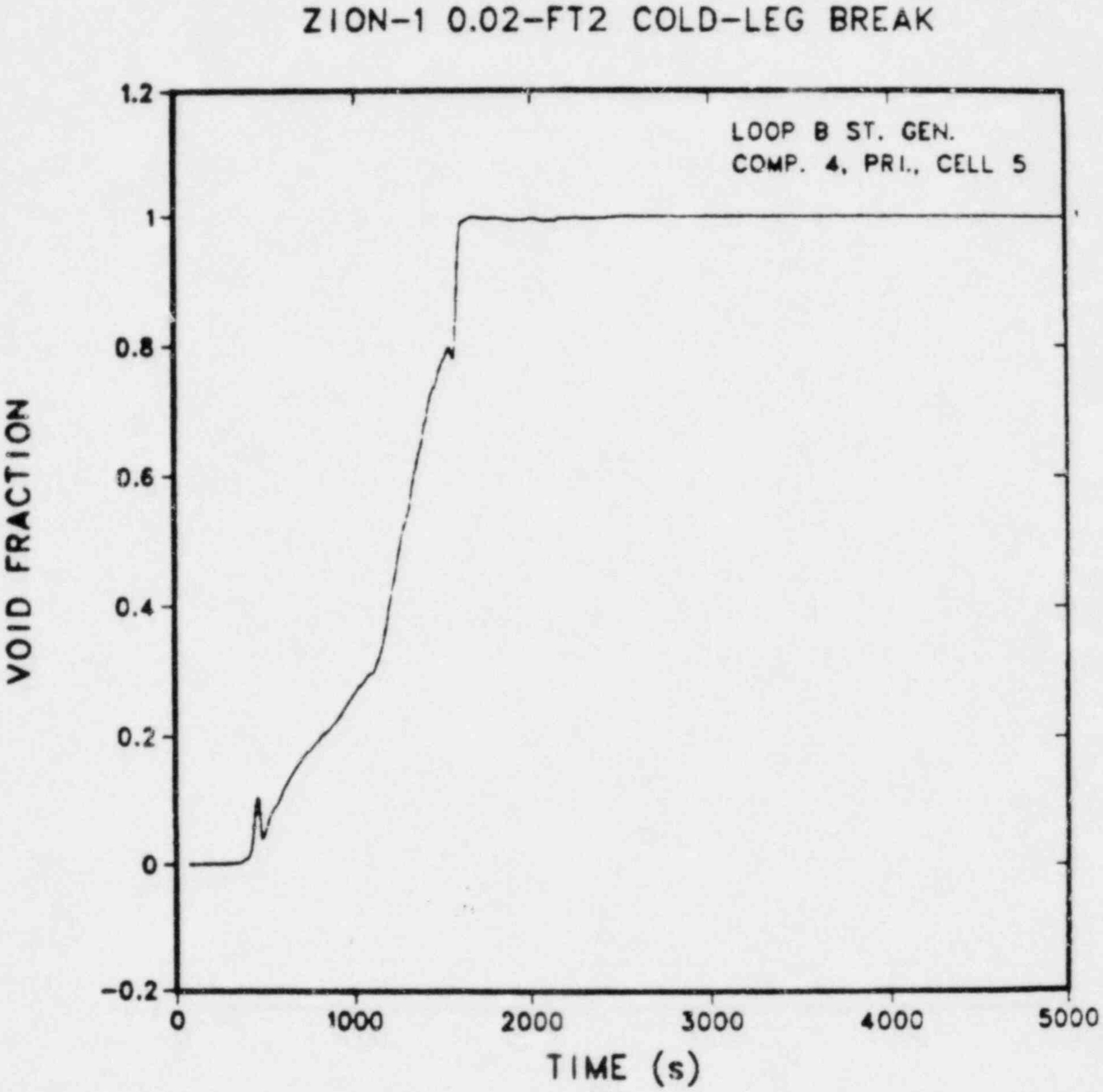

Fig. 18.
Loop B steam generator void fraction.

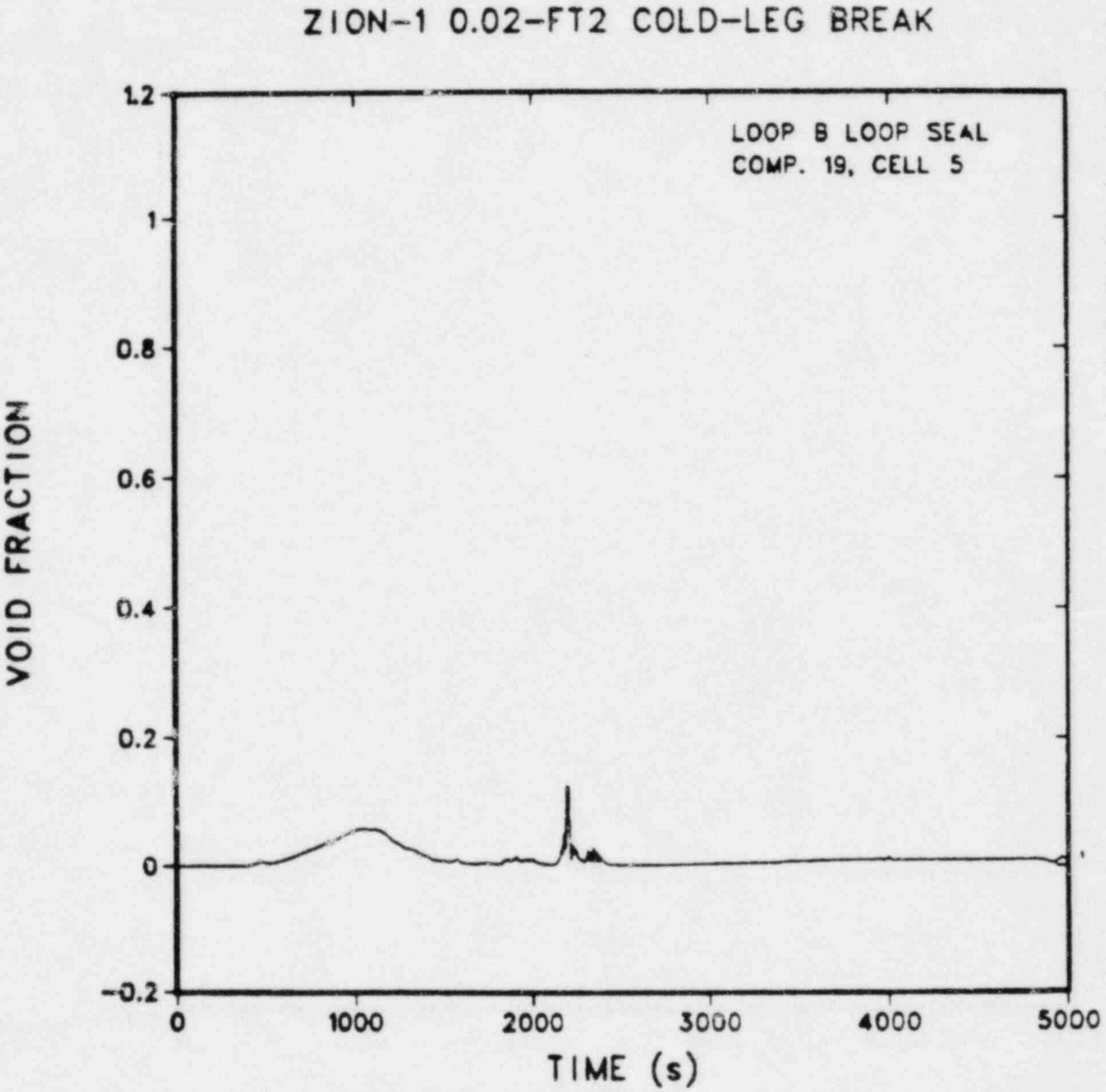

Fig. 19.
Loop B loop seal void fraction.

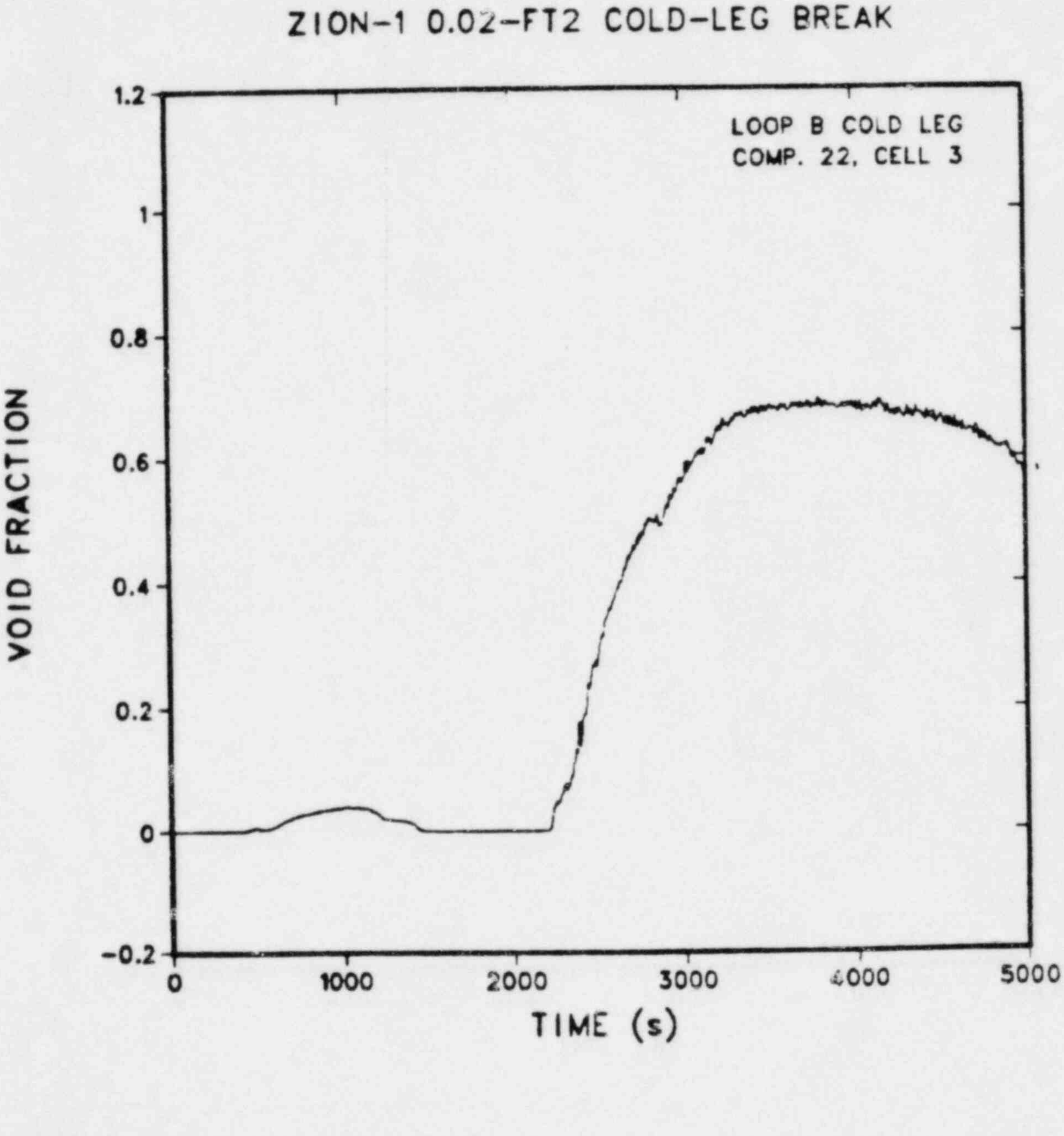

Fig. 20.
Loop B cold-leg void fraction.

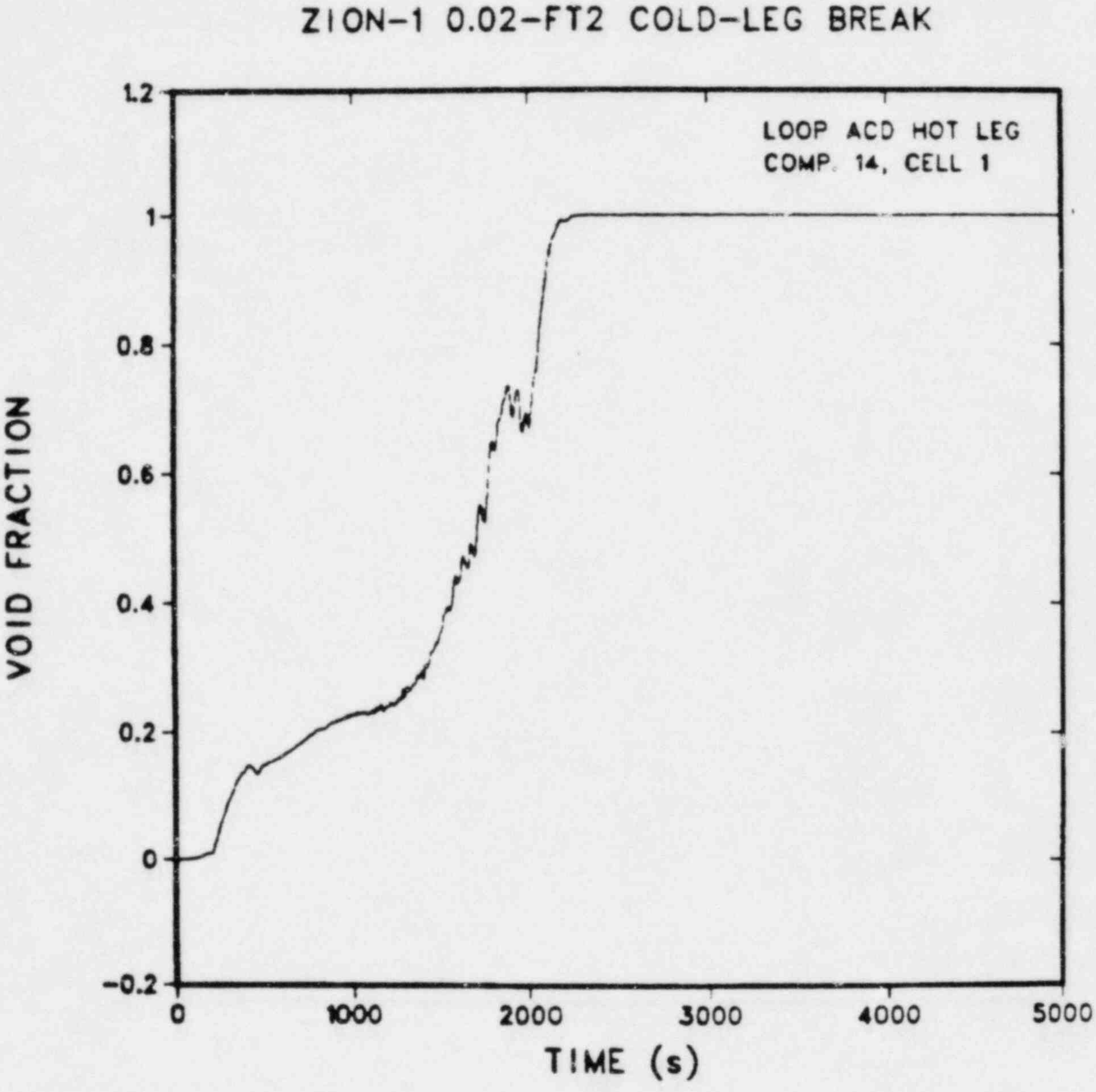

Fig. 21.
Loop ACD hot-leg void fraction.

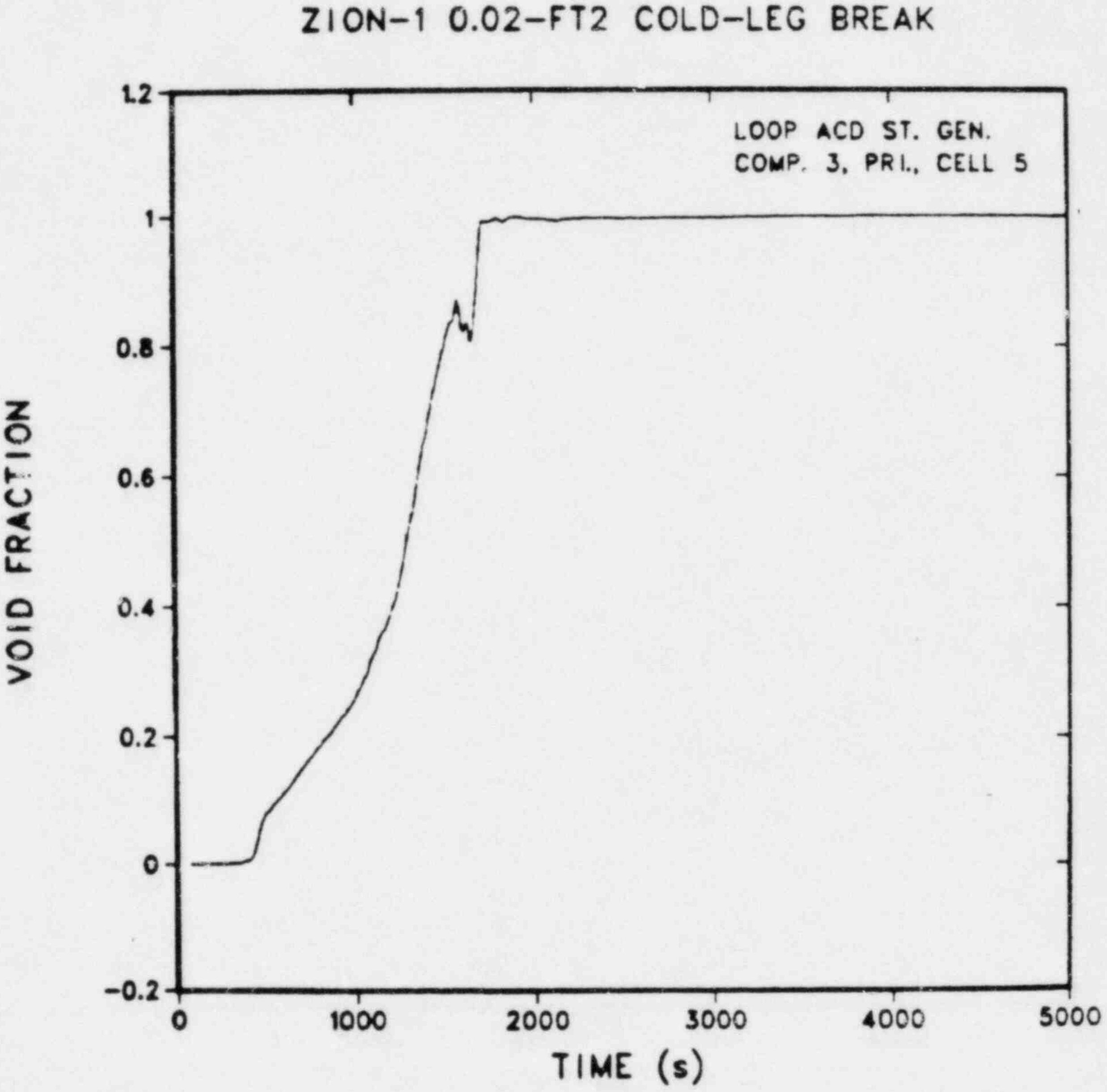

Fig. 22.
Loop ACD steam generator void fraction.

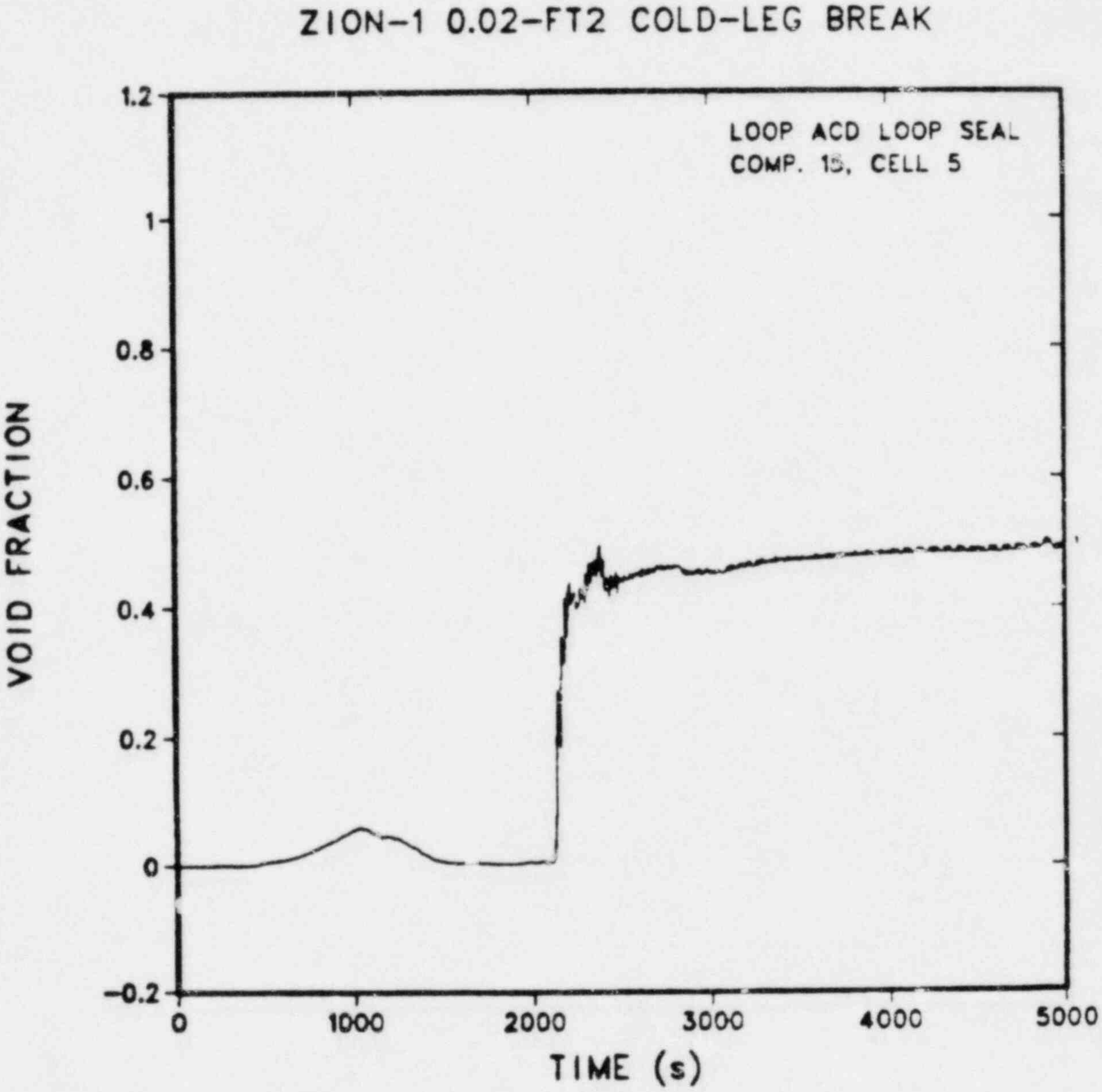

Fig. 23.
Loop ACD loop seal void fraction.

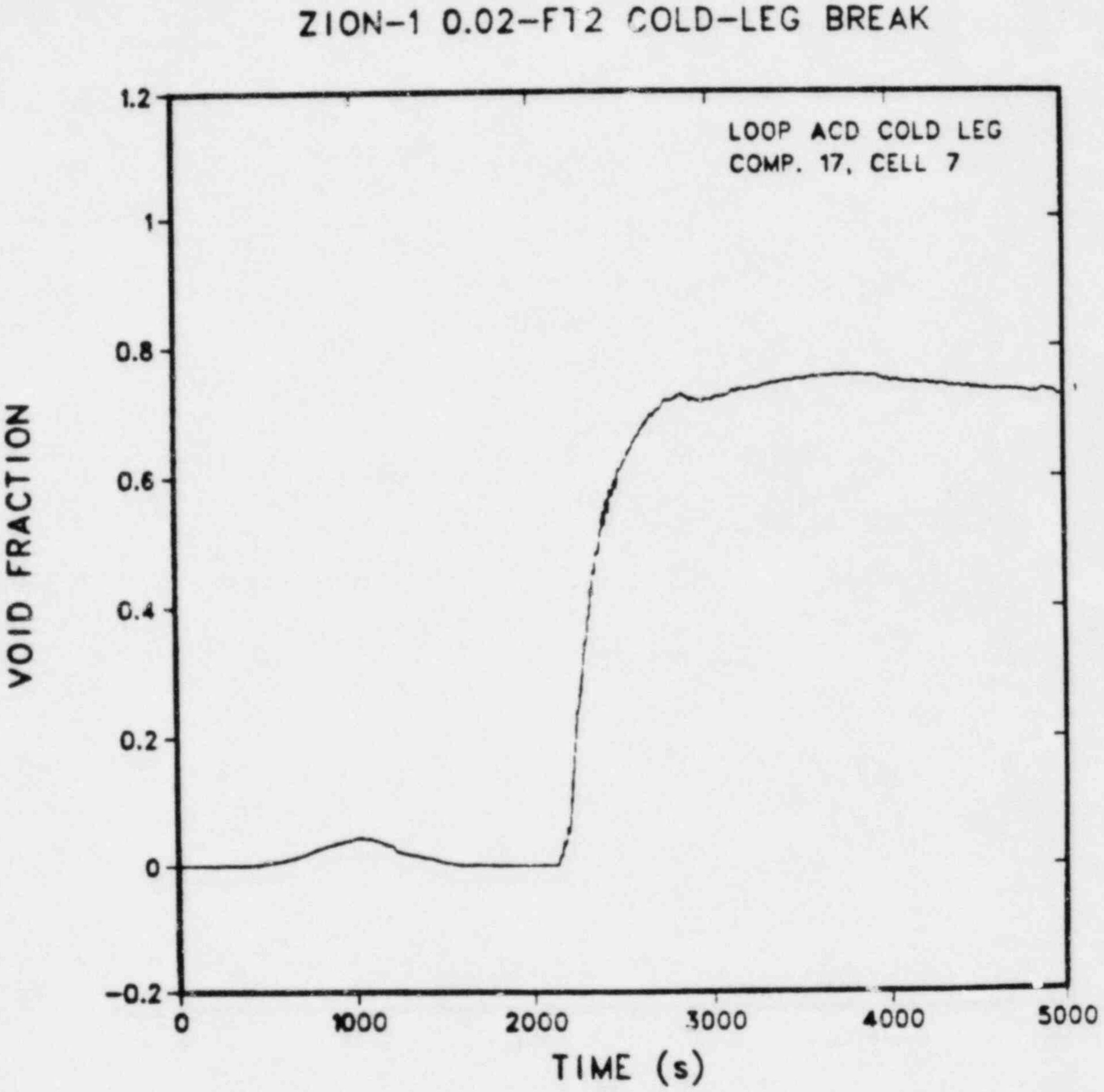

Fig. 24.
Loop ACD cold-leg void fraction.

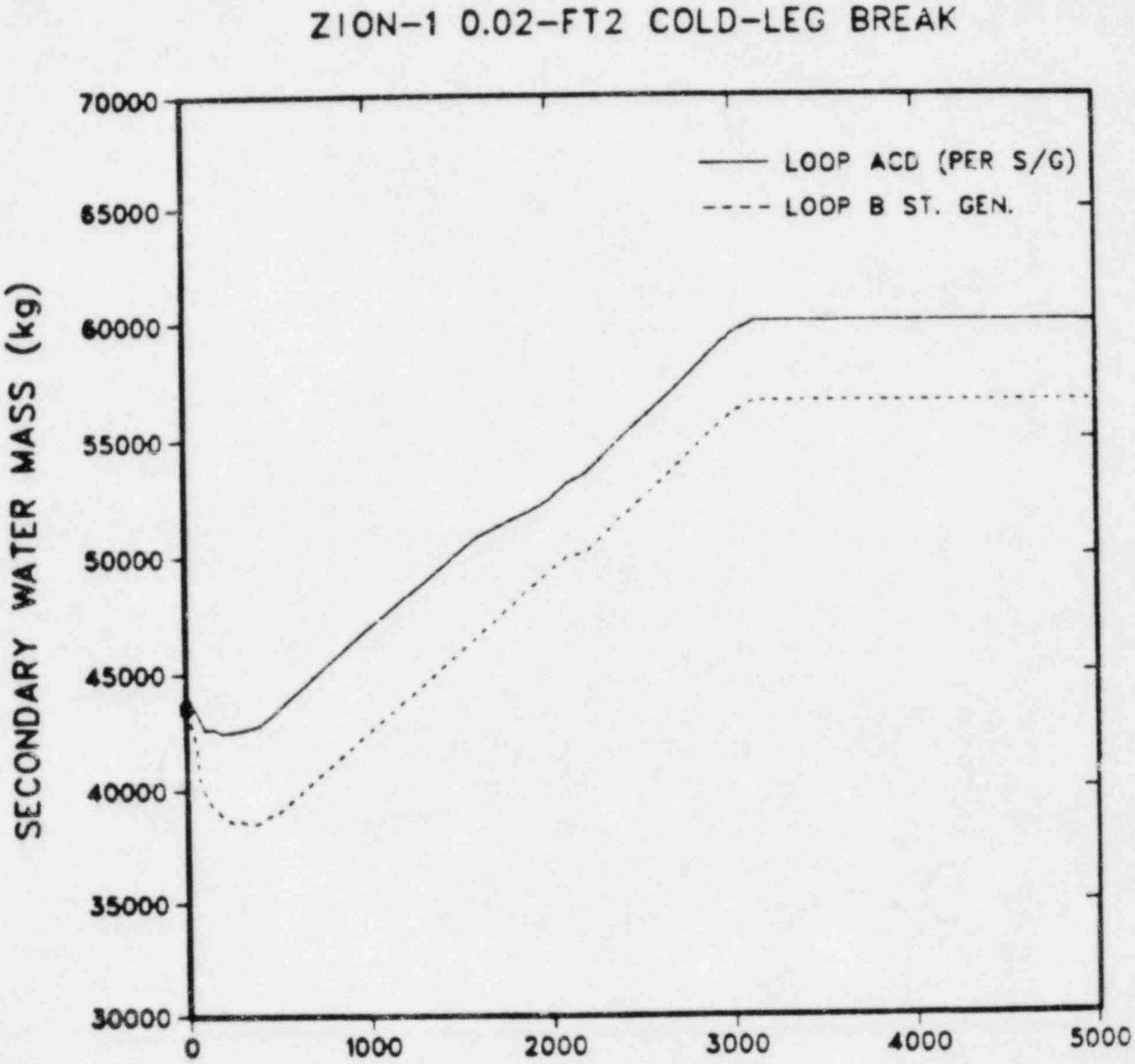

Fig. 25.
Steam generator secondary water mass inventory.

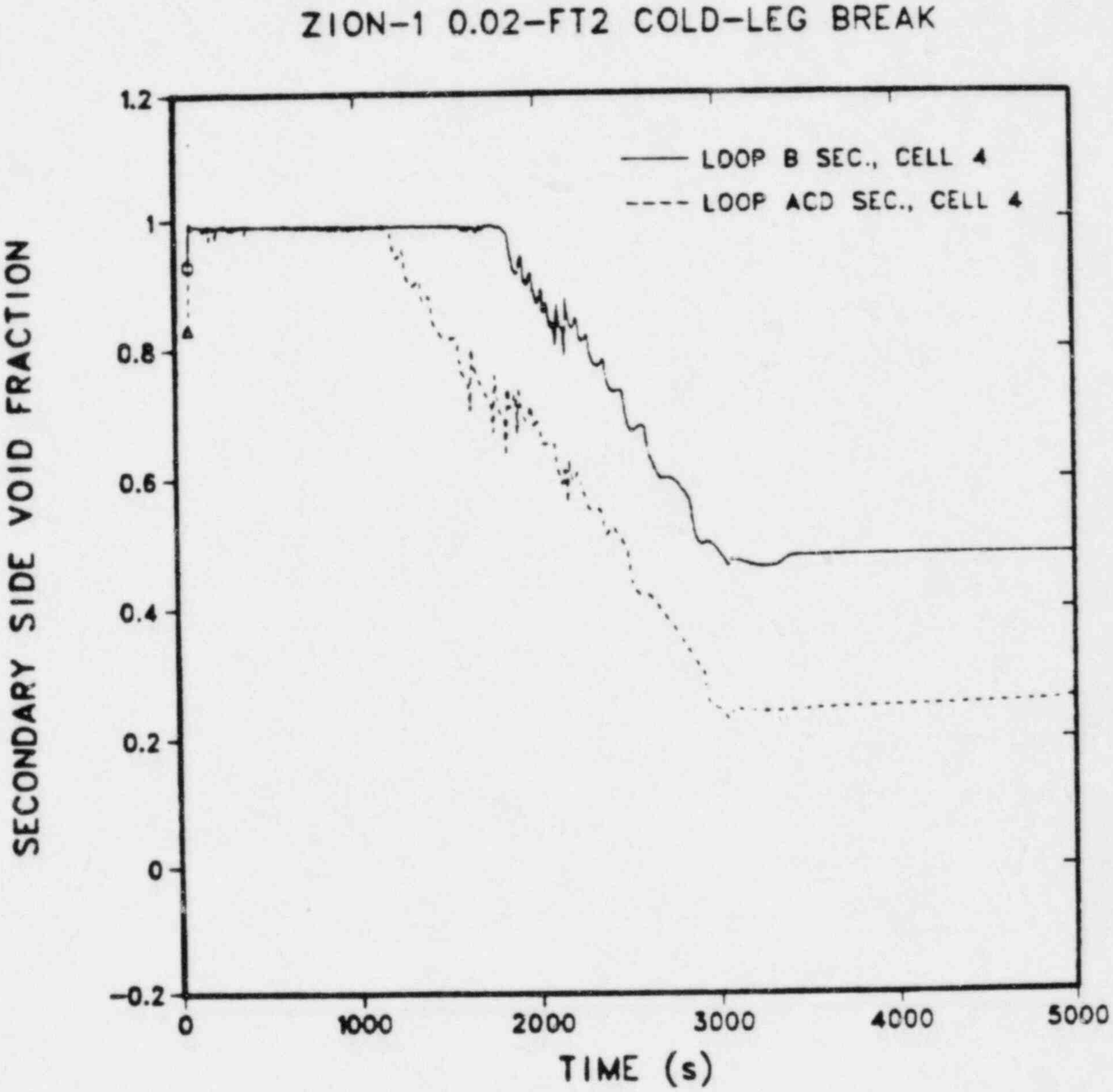

Fig. 26.
Steam generator void fraction at top of tube bundle.

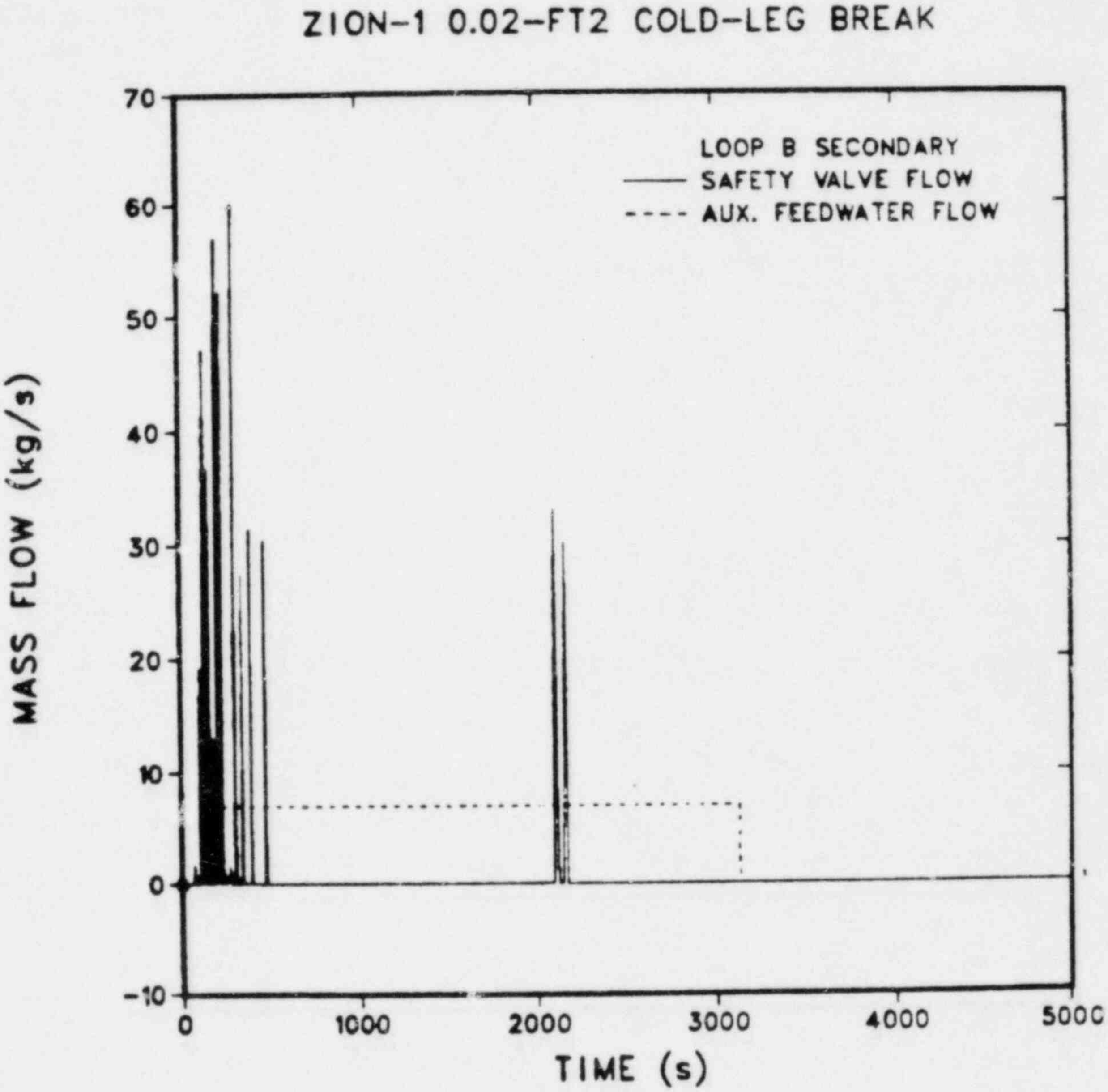

Fig. 27.
Loop B secondary safety valve and auxiliary feedwater flows.

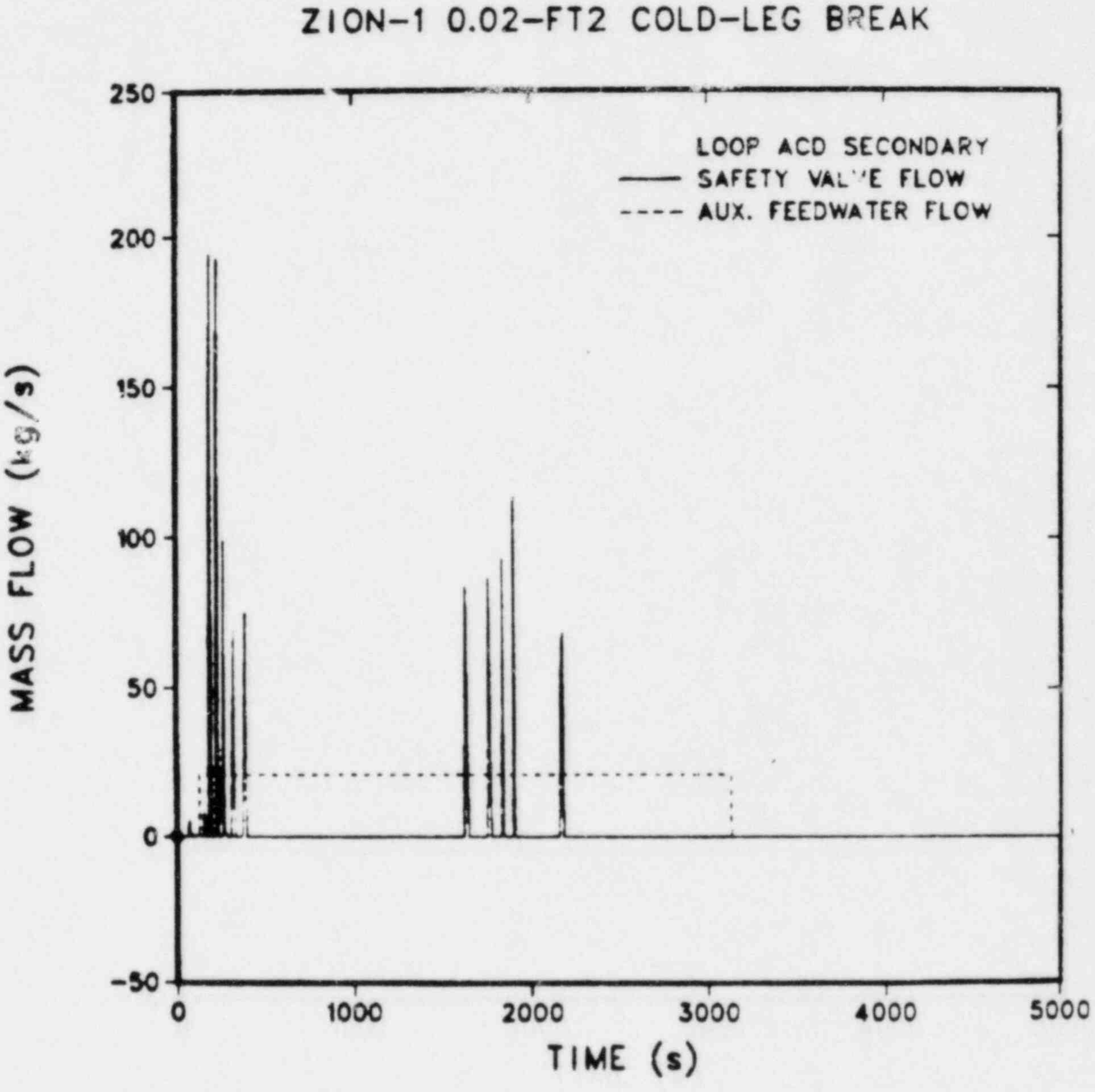

Fig. 28.
Loop ACD secondary safety valve and auxiliary feedwater flows.